

RECEIVED: January 12, 2021

ACCEPTED: April 7, 2021

PUBLISHED: May 14, 2021

In-medium modification of dijets in PbPb collisions at $\sqrt{s_{\text{NN}}} = 5.02 \text{ TeV}$



The CMS collaboration

E-mail: cms-publication-committee-chair@cern.ch

ABSTRACT: Modifications to the distribution of charged particles with respect to high transverse momentum (p_T) jets passing through a quark-gluon plasma are explored using the CMS detector. Back-to-back dijets are analyzed in lead-lead and proton-proton collisions at $\sqrt{s_{\text{NN}}} = 5.02 \text{ TeV}$ via correlations of charged particles in bins of relative pseudorapidity and angular distance from the leading and subleading jet axes. In comparing the lead-lead and proton-proton collision results, modifications to the charged-particle relative distance distribution and to the momentum distributions around the jet axis are found to depend on the dijet momentum balance x_j , which is the ratio between the subleading and leading jet p_T . For events with $x_j \approx 1$, these modifications are observed for both the leading and subleading jets. However, while subleading jets show significant modifications for events with a larger dijet momentum imbalance, much smaller modifications are found for the leading jets in these events.

KEYWORDS: Hadron-Hadron scattering (experiments), Jet physics, Quark gluon plasma

ARXIV EPRINT: [2101.04720](https://arxiv.org/abs/2101.04720)

Contents

1	Introduction	1
2	The CMS experiment	2
3	Event selection	3
4	Jet and track reconstruction	4
5	Jet to charged-particle angular correlations	5
6	Systematic uncertainties	7
7	Results	8
8	Summary	19
A	Dijet momentum balance migration matrices	21
	The CMS collaboration	25

1 Introduction

In relativistic heavy ion collisions, high transverse momentum (p_T) jets originate from partons that have undergone a hard scattering and may be used to probe the properties of the quark-gluon plasma (QGP) created in such collisions [1]. One phenomenon related to the properties of the QGP is parton energy loss [2], also known as jet quenching, which was first observed at the BNL RHIC [3, 4] and subsequently at the CERN LHC [5–8]. Jet quenching is seen as a suppression of high- p_T leading charged-particle and jet yields in heavy ion collisions relative to a proton-proton (pp) reference [9–12]. Using data collected at the LHC, studies have shown that the jet structure is also modified by the medium, as observed with measurements of the fragmentation functions [13, 14], and by the distribution of charged-particle p_T as a function of the radial distance from the jet axis [15]. These modifications are found to extend to large distances in relative pseudorapidity ($\Delta\eta$) and relative azimuth ($\Delta\varphi$) with respect to the jet axis [16–19]. Various theoretical models have attempted to account for these modifications [20–25] and while most models reproduce the modifications close to the jet axis, the large modifications observed far from the jet axis $\Delta r = \sqrt{(\Delta\varphi)^2 + (\Delta\eta)^2} > 0.5$ are not yet well modeled.

The analysis presented in this paper uses LHC data collected by the CMS experiment at a collision energy of $\sqrt{s_{\text{NN}}} = 5.02 \text{ TeV}$ in 2017 and 2018, corresponding to integrated luminosities of 320 pb^{-1} for pp and 1.7 nb^{-1} for lead-lead (PbPb) collisions, respectively.

Events are selected with nearly back-to-back ($\Delta\varphi > 5\pi/6$), high- p_T leading and subleading jet pairs. Correlations in relative pseudorapidity are measured for charged particles with respect to both the leading and subleading jet axes, where the relative azimuthal angle between the jet axes and charged particles is restricted to $|\Delta\varphi| < 1.0$. The “jet shape,” which is the distribution of charged-particle transverse momentum (p_T^{ch}) as a function of the distance from the jet axis Δr , is also studied. Results are presented differentially as functions of PbPb collision centrality (i.e., the degree of overlap of the colliding nuclei, with head-on collisions defined as “most central”) [7], p_T^{ch} , and dijet momentum balance $x_j = p_T^{\text{subleading}}/p_T^{\text{leading}}$. Compared to previous jet shape analyses in refs. [18, 19], the large PbPb data sample recorded in 2018 allows for differentiation in x_j for leading and subleading jet shapes extended to large distances from the jet axis.

2 The CMS experiment

The central feature of the CMS apparatus is a superconducting solenoid of 6 m internal diameter, providing a magnetic field of 3.8 T. Within the solenoid volume are a silicon pixel and strip tracker, a lead tungstate crystal electromagnetic calorimeter (ECAL), and a brass and scintillator hadron calorimeter (HCAL), each composed of barrel and two endcap sections. Two hadronic forward (HF) steel and quartz-fiber calorimeters complement the barrel and endcap detectors, extending the calorimeter from the range $|\eta| < 3.0$ provided by the barrel and endcap out to $|\eta| < 5.2$. The HF calorimeters are segmented to form 0.175×0.175 ($\Delta\eta \times \Delta\varphi$) towers. The sum of the transverse energies detected in the HF detectors ($3.0 < |\eta| < 5.2$) is used to define the event centrality in PbPb events and to divide the event sample into centrality classes, each representing a percentage of the total nucleus-nucleus hadronic interaction cross section. A detailed description of the centrality determination can be found in ref. [7].

Jets used in this analysis are reconstructed within the range $|\eta| < 1.6$. In the region $|\eta| < 1.74$, the HCAL cells have widths of 0.087 in both η and φ and thus provide high granularity. Within the central barrel region of $|\eta| < 1.48$, the HCAL cells map onto 5×5 ECAL crystal arrays to form calorimeter towers projecting radially outwards from the nominal interaction point. Within each tower, the energy deposits in ECAL and HCAL cells are summed to define the calorimeter tower energy.

The CMS silicon tracker measures charged-particle tracks within $|\eta| < 2.5$. It consists of 1856 silicon pixel and 15 148 silicon strip detector modules. Muons are measured in the pseudorapidity range $|\eta| < 2.4$, with detection planes made using three technologies: drift tubes, cathode strip chambers, and resistive plate chambers.

Events of interest are selected using a two-tiered trigger system. The first level (L1), composed of custom hardware processors, uses information from the calorimeters and muon detectors to select events at a rate of around 100 kHz [26]. The second level, known as the high-level trigger (HLT), consists of a farm of processors running a version of the full event reconstruction software optimized for fast processing, and reduces the event rate to around 1 kHz before data storage [27].

A detailed description of the CMS detector, together with a definition of the coordinate system used and the relevant kinematic variables, can be found in ref. [28].

3 Event selection

The pp and PbPb data are selected with a calorimeter-based HLT trigger that uses the anti- k_T jet clustering algorithm with a distance parameter of $R = 0.4$ [29]. The trigger requires events to contain at least one jet with $p_T > 80$ and $> 100\text{ GeV}$ for pp and PbPb collisions, respectively. For PbPb collisions, the underlying event contribution is subtracted from the jet p_T using an iterative method [30] before comparing to the threshold. The data sample selected by this trigger is referred to as “jet-triggered.” For the PbPb event selection, a minimum bias triggered [31] sample is also used in the analysis.

To reduce contamination from noncollision events, including calorimeter noise and beam-gas collisions, vertex and noise filters are applied offline to both the pp and PbPb data, following previous analyses of lower-energy data [6, 7]. These filters include requirements that at least three HF towers on either side of the interaction point have a tower energy above 3 GeV and that the vertex position along the beam line lies within 15 cm of the nominal interaction point. The average pileup (the number of collisions per beam bunch crossing) is about 2 in pp, and close to 1 in PbPb collisions. Because of the low pileup in the data samples, no pileup corrections are necessary.

Monte Carlo simulated event samples are used to evaluate the performance of the event reconstruction, particularly the track reconstruction efficiency, and the jet energy response and resolution. The hard scattering, parton shower, and fragmentation of the partons are modeled using the PYTHIA 8 event generator with tune CP5 [32, 33]. The specific PYTHIA version used is 8.226 and the parton distribution function set is NNPDF3.1 at next-to-next-to-leading order [34]. The CMS detector response is simulated using the GEANT4 toolkit [35]. The soft underlying event for the PbPb collisions is simulated by the HYDJET 1.9 event generator [36]. The energy density in the HYDJET simulation is tuned to match the data by shifting the centrality binning in standard HYDJET simulation by 5 percentage points upwards. This tuning is based on a random cone study, where rigid cones with a radius 0.4 are placed in random directions in events, and the energy densities in the cones are determined by summing the particle transverse momenta within the cone. The above tuning provides the best agreement in random cone energy densities between data and HYDJET. To simulate jet events in PbPb collisions, PYTHIA 8 generated hard events are embedded into soft HYDJET events. This sample is denoted as PYTHIA+HYDJET.

In PbPb collisions, jets are produced more frequently in central events than in non-central events because of the large number of binary collisions per nuclear interaction. A centrality-based reweighting is applied to the PYTHIA+HYDJET sample in order to match the centrality distribution of the jet-triggered PbPb data. An additional reweighting procedure is performed to match the simulated vertex distributions to data for both the pp and PbPb samples.

The event selection works as follows. First, the two jets with highest p_T are located in the range of $|\eta| < 2$. The highest p_T jet is called the leading jet and it is required to pass a

p_T cut of $p_{T,1} > 120 \text{ GeV}$. The second highest p_T jet is termed the subleading jet and for it a cut $p_{T,2} > 50 \text{ GeV}$ is applied. Then, the back-to-back requirement, a condition demanding that the jet separation in φ obeys $\Delta\varphi_{1,2} > 5\pi/6$ is enforced. Finally, both jets are required to fall within $|\eta| < 1.6$ to ensure the most stable jet reconstruction performance and to allow for good tracker acceptance on both sides of the jets. There is no veto for additional jets in the event. The events containing such pairs of back-to-back jets are referred as dijet events for the remainder of the paper.

4 Jet and track reconstruction

For this analysis, jets in both pp and PbPb collisions are reconstructed using the anti- k_T algorithm with a distance parameter $R = 0.4$, as implemented in the FASTJET framework [37]. A particle flow (PF) algorithm using an optimized combination of information from various elements of the CMS detector is used to reconstruct leptons, photons, and charged and neutral hadrons [38]. These PF candidates are employed to reconstruct the jets used in this analysis. The jets are first clustered using E-scheme clustering [37] and the jet axis is recalculated with the winner-take-all algorithm [39, 40] using anti- k_T and the same constituents. In the E-scheme clustering, particle pairs are iteratively combined to form pseudo-jets (an object that is a combination of particles or other pseudo-jets), with the direction of the new pseudo-jet given by the sum of the four-momenta of the particles. In the winner-take-all scheme, the direction of the new pseudo-jet in each iteration is aligned with the direction of the particle or pseudo-jet with higher p_T . It follows that the E-scheme axis for the final jet is given by the sum of pseudo-jet four-momenta, while the winner-take-all axis is determined by the axis of the hardest pseudo-jet. The winner-take-all axis is preferred in this analysis over the default E-scheme axis because of an artificial feature created by the E-scheme axis that results in a strong depletion of particles just outside of the jet cone radius. Not having to correct for this feature leads to smaller uncertainties.

In order to subtract the soft underlying event contribution to the jet energy in PbPb collisions, a constituent subtraction method [41] is employed. This involves a particle-by-particle approach that corrects jet constituents based on the local average underlying event density. The energy density is estimated using an event-by-event, iterative algorithm [30] that finds the mean value, $\langle E_{\text{PF}} \rangle$, and dispersion, $\sigma(E_{\text{PF}})$, of the energies from the PF candidates in η strips [6, 7]. In pp collisions, where the underlying event level is negligible, jets are reconstructed without underlying event subtraction.

The track reconstruction used in pp and PbPb collisions is described in ref. [42]. For the charged-particle tracks used in jet to charged-particle correlations, it is required that the relative p_T uncertainty of each track is less than 10%. In PbPb collisions, tracks must also have at least 11 hits in the tracker layers and satisfy a stringent fit quality requirement, specifically that the χ^2 , divided by the product of the number of fit degrees of freedom and the number of tracker layers hit, be less than 0.18. Furthermore, it is required that the significance of the distance of closest approach of a charged-particle track to at least one primary vertex in the event is less than 3 standard deviations. This is done to decrease

x_j	0–10%	10–30%	30–50%	50–90%	pp
$0 < x_j < 1$	5.8×10^5	6.6×10^5	2.6×10^5	0.78×10^5	110×10^5
$0 < x_j < 0.6$	40%	35%	29%	26%	24%
$0.6 < x_j < 0.8$	33%	34%	36%	35%	36%
$0.8 < x_j < 1$	27%	31%	35%	39%	40%

Table 1. The total number of events for pp and for different PbPb centrality bins are shown in the top row. The other rows show the percentage of all events that falls within a given x_j bin.

the likelihood of counting nonprimary charged particles originating from secondary decay products, and is applied for both pp and PbPb collisions. Finally, for PbPb collisions a selection based on the relationship of a track to the calorimeter energy deposits along its trajectory is applied in order to reduce the contribution of misreconstructed tracks with very high p_T . Tracks with $p_T > 20$ GeV are required to have an associated energy deposit of at least half of their momentum in the CMS calorimeters. Corrections for tracking efficiency, detector acceptance, and misreconstruction rate are obtained and applied following the procedure of ref. [43].

5 Jet to charged-particle angular correlations

Correlations between reconstructed jets and charged-particle tracks are studied by forming a two-dimensional distribution of $\Delta\eta$ and $\Delta\varphi$ of the charged particles relative to the jet axis. Events in PbPb collisions are divided into four centrality intervals, 0–10, 10–30, 30–50, and 50–90%, based on the total energy collected in the HF calorimeter [7]. The events are also binned by the charged-particle p_T with bin boundaries of 0.7, 1, 2, 3, 4, 8, 12, and 300 GeV and in the dijet momentum balance x_j with bin boundaries of 0, 0.6, 0.8, and 1. The effects of jet energy resolution to the x_j binning are explored in appendix A. The two-dimensional correlation histograms are filled by correlating all charged particles in the event with the leading jet and the subleading jet, separately. For the jet shape measurement, each entry is weighted by the charged particle p_T value. The histograms are then normalized by the number of dijets. The numbers of dijets in the data samples for each x_j and centrality bin are summarized in table 1.

Since the detector has limited acceptance in η , it is more probable to find jet-charged-particle pairs with small rather than large $\Delta\eta$ values. Thus, the raw correlations have a shape where the charged-particle yield strongly decreases toward large $\Delta\eta$. A mixed-event method is employed to correct for these detector acceptance effects. In this method, the jet and charged particles from different events are mixed to ensure that no physical correlations exist in the resulting distribution. What is left is the structure arising from the detector acceptance. When the mixed events are constructed, it is required that the primary vertex positions along the beam axis match within 0.5 cm and that the centrality values match within 0.5 percentage points between the two events. For pp collisions, a jet-triggered sample is used for the mixed events, while for PbPb collisions a minimum bias sample is used to properly capture the long range correlations. This procedure is similar to that used in previous analyses [18, 19]. Denoting the number of dijets satisfying the selection criteria

as N_{dijet} , the per-dijet associated charged-particle yield corrected for the acceptance effects is given by

$$\frac{1}{N_{\text{dijet}}} \frac{d^2 N}{d\Delta\eta d\Delta\varphi} = \frac{ME(0,0)}{ME(\Delta\eta,\Delta\varphi)} S(\Delta\eta,\Delta\varphi), \quad (5.1)$$

where N is the number of jet-particle pairs, the signal pair distribution $S(\Delta\eta,\Delta\varphi)$ represents the per-dijet normalized yield of jet-particle pairs from the same event,

$$S(\Delta\eta,\Delta\varphi) = \frac{1}{N_{\text{dijet}}} \frac{d^2 N^{\text{same}}}{d\Delta\eta d\Delta\varphi}, \quad (5.2)$$

and the mixed-event pair distribution $ME(\Delta\eta,\Delta\varphi)$ is given by

$$ME(\Delta\eta,\Delta\varphi) = \frac{d^2 N^{\text{mixed}}}{d\Delta\eta d\Delta\varphi}. \quad (5.3)$$

The ratio $ME(0,0)/ME(\Delta\eta,\Delta\varphi)$ is the normalized correction factor. The maximum of the mixed event distribution can be found at $(0,0)$ as no pairs with $\Delta\eta = 0$ are lost as a consequence of acceptance effects.

The acceptance-corrected distribution has contributions from several sources. The jet correlation shows up as a Gaussian peak around $(\Delta\eta,\Delta\varphi) = (0,0)$ together with a peak elongated in $\Delta\eta$ around $\Delta\varphi = \pi$. While the underlying event contribution to jet energy and momentum is corrected for as previously discussed in section 4, the underlying event particles paired with the jet remain within the acceptance-corrected distribution, and thus have to be removed. To model this background, the $\Delta\varphi$ distribution is averaged over the region $1.5 < |\Delta\eta| < 2.5$ on the near side ($|\Delta\varphi| < \pi/2$) of the jet. The same background region criteria are used for correlations of charged particles with both leading and subleading jets and the backgrounds are combined to cover the full $\Delta\varphi$ range. This procedure is applied to avoid an “eta swing” effect. Momentum conservation dictates that in a statistical ensemble of dijets, the two jets must be approximately back-to-back in $\Delta\varphi$, but no such requirement exists for the $\Delta\eta$ separation. Thus, the away side ($|\Delta\varphi| > \pi/2$) jet peak is prolonged in $\Delta\eta$ in jet to charged-particle correlation distributions. To avoid mixing the jet signal with the background, the away side region needs to be avoided in the background estimation. The background determined using the respective near-side components is propagated to the full $(\Delta\eta,\Delta\varphi)$ plane and subtracted from the acceptance-corrected distribution to obtain the jet signal.

Finally, simulation-based corrections are applied to account for a bias toward selecting jets with a harder constituent p_T spectrum (affecting PbPb and pp events similarly) and a bias toward selecting jets that are affected by upward fluctuations in the soft underlying event yield (relevant for PbPb events only). Jets with a harder constituent p_T spectrum are more likely to be successfully reconstructed than jets with a softer p_T spectrum because the calorimeter response does not scale linearly with the incident particle energy, resulting in a bias toward the selection of jets with fewer associated particles. A residual correction for this bias is derived and applied following the method described in refs. [16–18], by comparing per-jet yields of generated particles correlated to reconstructed jets relative to those correlated to generated jets. This correction is derived using a PYTHIA 8 simulation for pp events and considering only generated particles coming from the embedded PYTHIA hard process in PYTHIA+HYDJET simulation for PbPb events.

For PbPb events, there is an additional jet reconstruction bias toward the selection of jets that are produced in the vicinity of upward fluctuations in the underlying event background. The underlying event fluctuations together with a steeply falling jet p_T spectrum produce a resolution effect on the jet energy scale. This causes more jets associated with upward fluctuations than with downward fluctuations of the underlying event to pass the analysis threshold. To account for this bias, a similar procedure to that outlined in refs. [17, 18, 44] is followed. Correlations in the PYTHIA+HYDJET sample between reconstructed jets and generated particles are constructed using only particles from the HYDJET underlying event, excluding those from the embedded hard process. This gives an estimate of the underlying event yield on top of which the jet correlations are found in the data. To reduce the fluctuations in the generated sample, the obtained distribution is symmetrized in $\Delta\eta$ and $\Delta\varphi$, before being applied as a correction to the PbPb data.

6 Systematic uncertainties

The following sources of uncertainty are considered in this analysis:

- *Underlying event fluctuation bias.* This source accounts for uncertainties in correcting for the jet reconstruction bias resulting from upwards fluctuations of the underlying event background. Three different causes are considered. The first is a potential difference between the quark and gluon jet fraction in simulation and in data. The potential difference is estimated to be less than 25% using a template fit to the multiplicity distribution of PF candidates within the jet cone in the data. Then the uncertainty is estimated by varying the quark/gluon jet fraction in simulation by this amount. The second source considers the difference in the underlying event energy density between simulation and data, and is estimated by random cone studies. The uncertainty is determined by varying the centrality binning of the HYDJET simulation by 1 percentage point around the best match to data, which is the range giving a reasonable agreement. Finally, there is the uncertainty in the underlying event level for the simulation from which the underlying event fluctuation bias correction is derived. This uncertainty is obtained in a similar manner as for data, as discussed below in the “underlying event subtraction” bullet point.
- *Jet fragmentation bias.* Most of the detector and resolution effects contributing to the jet fragmentation bias uncertainty arise from the uncertainty in the ratios of quark and gluon jets between data and simulation, as discussed for the underlying event fluctuation bias above. Deriving the corrections separately for quark and gluon jets and varying their relative contribution within the estimated difference between data and Monte Carlo, a 10% variation in the fragmentation bias correction is observed. This difference is assigned as a systematic uncertainty.
- *Jet energy scale.* These uncertainties are estimated by varying the jet energy corrections within their uncertainties and seeing how these changes affect the final correlations. The uncertainties of the jet energy corrections are discussed in detail in ref. [45].
- *Jet energy resolution.* This uncertainty is estimated by adding a Gaussian spread to the nominal jet energies such that the jet energy resolution estimated from the

simulation is worsened by 20% and comparing the obtained results to the nominal ones. The value of 20% comes from the maximal estimated difference in the jet energy resolution between data and simulation.

- *Trigger bias.* The calorimeter-based trigger with a threshold of 100 GeV is not fully efficient for the PbPb collisions. To see if this has an effect on the final results, the analysis was repeated requiring a prescaled trigger with a threshold of 80 GeV and the results with this trigger were compared to the nominal ones. For the leading jet shapes, it was found that there is a 2% yield difference in the bin closest to the jet axis, while for the other bins and for the subleading jets the difference is negligible. The 2% difference is therefore applied as a systematic uncertainty on the first bin. The trigger used for the pp collisions is fully efficient and thus has no trigger bias uncertainty.
- *Tracking efficiency.* Two sources of uncertainty are considered. First, there are possible track reconstruction differences in data and simulation. Following the method in ref. [43], it is estimated that the uncertainty in the track reconstruction efficiency and misidentification rate corrections is 5% for PbPb and 2.4% for pp collisions. Second, the ratio of corrected reconstructed yields to generator level yields is studied for PYTHIA 8 and PYTHIA+HYDJET simulations. It is found that the reconstructed and generated yields match within 3% in PbPb and 1% in pp collisions, and these numbers are used as a systematic uncertainty from this source. An extra uncertainty is added to tracks close to the jet axis, as in the high multiplicity environment around the jet, the tracking efficiency is found to be 1–2% worse than far away from the jets.
- *Acceptance correction.* In an ideal case, the mixed-event corrected jet to charged-particle angular distribution contains a jet peak and an uncorrelated underlying event background. Since jet correlations are small angle correlations, the underlying event is expected to dominate far from the jet axis (sideband), and thus the distribution at $|\eta| > 1.5$ should be uniform. To evaluate possible deviations from the uniformity, a constant function is separately fit to each sideband region of the acceptance-corrected $\Delta\eta$ distribution ($-2.5 < \Delta\eta < -1.5$ and $1.5 < \Delta\eta < 2.5$). The difference between the average yield in the positive and negative sides determined this way is assigned as a systematic uncertainty.
- *Underlying event subtraction.* Uncertainties resulting from the underlying event subtraction are determined by considering the two parts of the sideband region, $1.5 < |\Delta\eta| < 2.0$ and $2.0 < |\Delta\eta| < 2.5$, after the underlying event subtraction. The average yield is calculated in each of the regions and the larger deviation from zero is assigned as a systematic uncertainty.

The total systematic uncertainties are obtained by adding all the individual components together in quadrature. For the leading and subleading jet correlations, the uncertainties integrated over x_j and Δr are listed in tables 2 and 3, respectively.

7 Results

Figure 1 shows the results for charged-particle yields in the region $|\Delta\varphi| < 1$ as a function of $|\Delta\eta|$ from the leading jets. The intervals in track p_T are indicated by the stacked

Source	0–10%	10–30%	30–50%	50–90%	pp
Underlying event fluctuation bias	<4%	<3%	<2%	<1%	—
Jet fragmentation bias	<3%	<2%	<2%	<2%	<1%
Residual jet energy scale	3–7%	3–8%	3–8%	3–9%	1–9%
Jet energy resolution	1–3%	1–3%	1–3%	1–3%	<2%
Trigger bias	<2%	<2%	<2%	<2%	—
Tracking efficiency	6–8%	6–8%	6–7%	6–7%	3%
Acceptance correction	<3%	<3%	<3%	<3%	<1%
Underlying event subtraction	<4%	<3%	<3%	<3%	<2%
Total	8–14%	8–12%	8–12%	8–11%	3–10%

Table 2. Systematic uncertainties for the leading jet shape components, integrated over x_j , and Δr , and shown for pp and centrality-binned PbPb collisions. The ranges correspond to the p_T dependence of the uncertainty. If some p_T bins have an uncertainty smaller than 0.5%, the range is presented with a “<” symbol and the upper bound.

Source	0–10%	10–30%	30–50%	50–90%	pp
Underlying event fluctuation bias	<1%	<1%	<1%	<1%	—
Jet fragmentation bias	<3%	<2%	<1%	<1%	<1%
Residual jet energy scale	2–9%	2–9%	2–10%	2–10%	1–11%
Jet energy resolution	1–3%	1–2%	1–2%	1–2%	1%
Tracking efficiency	6%	6%	6%	6%	3%
Acceptance correction	<1%	<1%	<1%	<1%	<1%
Underlying event subtraction	<3%	<3%	<3%	<3%	<3%
Total	7–11%	7–11%	7–11%	7–11%	4–11%

Table 3. Systematic uncertainties for the subleading jet shape components, integrated over x_j , and Δr , and shown for pp and centrality-binned PbPb collisions. The ranges correspond to the p_T dependence of the uncertainty. If some p_T bins have an uncertainty smaller than 0.5%, the range is presented with a “<” symbol and the upper bound.

histograms. The first row shows the charged-particle yields without any selection on x_j , while other rows show the charged-particle yields in different bins of x_j from the most unbalanced $0 < x_j < 0.6$ (second row) to the most balanced $0.8 < x_j < 1.0$ (fourth row) dijet events. The first panel in each row shows the charged-particle yields for the pp collisions while other panels show the same yields for the PbPb collisions in different centrality bins, from the most peripheral 50–90% (second panel) to the most central 0–10% (fifth panel) collisions. Measurements of the per-jet invariant charged-particle yields show an enhancement of these yields in PbPb relative to pp collisions. The enhancement is greatest for central collisions and decreases for more peripheral collisions. Comparing the different x_j bins, the enhancement of the total PbPb yield relative to pp yield is seen to increase slightly as the dijet momenta become more balanced. A geometrical bias could explain this, as discussed, for example, in ref. [46], since it can result in different path lengths inside the medium for the leading and subleading jets. In balanced dijet events, both jets lose significant amounts of energy, while in events with unbalanced dijet momenta,

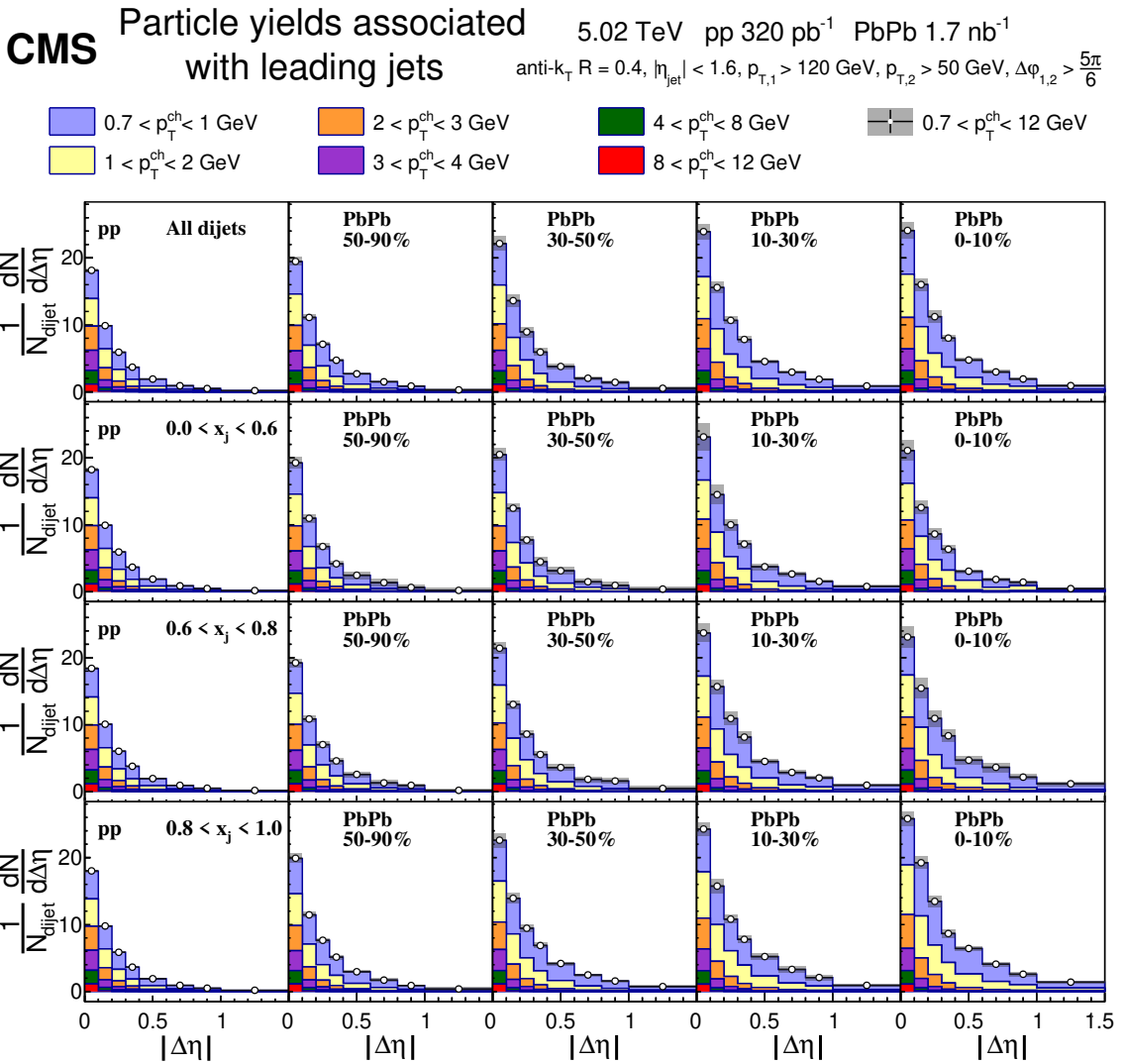


Figure 1. Distributions of charged-particle yields correlated to leading jets in the region $|\Delta\varphi| < 1$ as a function of $|\Delta\eta|$ for pp (first column) and PbPb (second to fifth columns) collisions in different centrality bins, shown differentially for all p_{T}^{ch} bins. The first row shows the charged-particle yields without any selection on x_j , while other rows show the charged-particle yields in different bins of x_j , starting with the most unbalanced $0 < x_j < 0.6$ (second row) to the most balanced $0.8 < x_j < 1.0$ (fourth row) dijet events.

the leading jet is most likely produced closer to the surface of the plasma, thus losing less energy. The x_j trend in PbPb collisions could also be influenced by energy loss fluctuations, as studied in ref. [47].

Figure 2 shows the results for charged-particle yields in the region $|\Delta\varphi| < 1$ presented differentially in p_{T}^{ch} , as a function of $|\Delta\eta|$ for the subleading jets. The results are arranged in the same manner as for leading jets in figure 1. As with the leading jets, the measurements of the per-jet invariant charged-particle yields for subleading jets show an enhancement in PbPb relative to pp collisions, with the greatest enhancement observed for central collisions.

The magnitude of this enhancement is larger than for the leading jets in figure 1 (note the different vertical scales between the two figures). Comparing the different x_j bins for the subleading jets, the enhancement of the total PbPb yield relative to the pp yield is seen to slightly decrease as the dijet momenta become more balanced. This is opposite to the trend found for the leading jets and may reflect the greater path length through the plasma taken by the subleading jets for more unbalanced dijet events. When comparing leading and subleading results, there also might be an effect where the selection of leading and subleading jets in PbPb collisions is reversed as a consequence of parton energy loss in quark-gluon plasma.

The jet radial momentum distributions $P(\Delta r)$ and jet shapes $\rho(\Delta r)$ are studied by examining the distribution of charged particles in annular rings of width $\delta r = 0.05$ around the jet axis. The jet radial momentum profile $P(\Delta r)$ is the transverse momentum weighted distribution of particles around the jet axis:

$$P(\Delta r) = \frac{1}{\delta r} \frac{1}{N_{\text{jets}}} \sum_{\text{jets}} \sum_{\text{tracks} \in (\Delta r_a, \Delta r_b)} p_T^{\text{ch}}, \quad (7.1)$$

where Δr_a and Δr_b define the annular edges of Δr , and $\delta r = \Delta r_b - \Delta r_a$. The jet shape $\rho(\Delta r)$ is the momentum distribution normalized to unity over $\Delta r < 1$, with

$$\rho(\Delta r) = \frac{P(\Delta r)}{\sum_{\text{jets}} \sum_{\text{tracks} \in \Delta r < 1} p_T^{\text{ch}}}. \quad (7.2)$$

The main difference between these two is that while jet shapes focus exclusively on studying the shape of the distribution, jet radial momentum distributions are sensitive to changes in the absolute scale of the in-jet momentum flow between pp and PbPb collisions.

Figure 3 shows the jet radial momentum distributions in PbPb and pp collisions differentially in p_T^{ch} . The first row shows the jet radial momentum distribution for the leading jets, while the second row is for subleading jets. The first panel in each row shows the results for pp collisions, while other panels are for PbPb collisions in different centrality bins, starting from the most peripheral 50–90% (second panel) to the most central 0–10% (fifth panel) collisions. For both leading and subleading jets, when going toward more central events, the momentum profile at large Δr is enhanced in PbPb collisions over the one in pp collisions. The enhancement is largest for the low- p_T charged particles, as expected if the energy lost at high p_T resulting from interactions of partons with the quark-gluon plasma reappears in the form of low- p_T particles far away from the jet axis.

Figure 4 shows the PbPb to pp collision ratio of the jet radial momentum profiles for different centrality bins. A clear trend can be seen in these plots. The enhancement of the PbPb radial momentum distribution over the pp distribution is the largest for the most central collisions and for larger separations of the charged particles from the jet axis. The enhancement for subleading jets is not as large as for the leading jets because of the widening of the pp reference distribution. The main reason of this widening is the fact that subleading jets have significantly lower p_T compared to leading jets, and jet shapes for lower p_T jets are wider.

The jet shape results for the leading jets are presented in figure 5. The first row shows the jet shape without any selection on x_j , while other rows show the jet shape in different x_j bins. The first panel in each row shows the jet shape for pp collisions. Without x_j selection, about 3.7% of the total charged-particle constituent p_T is out-of-cone ($R > 0.4$).

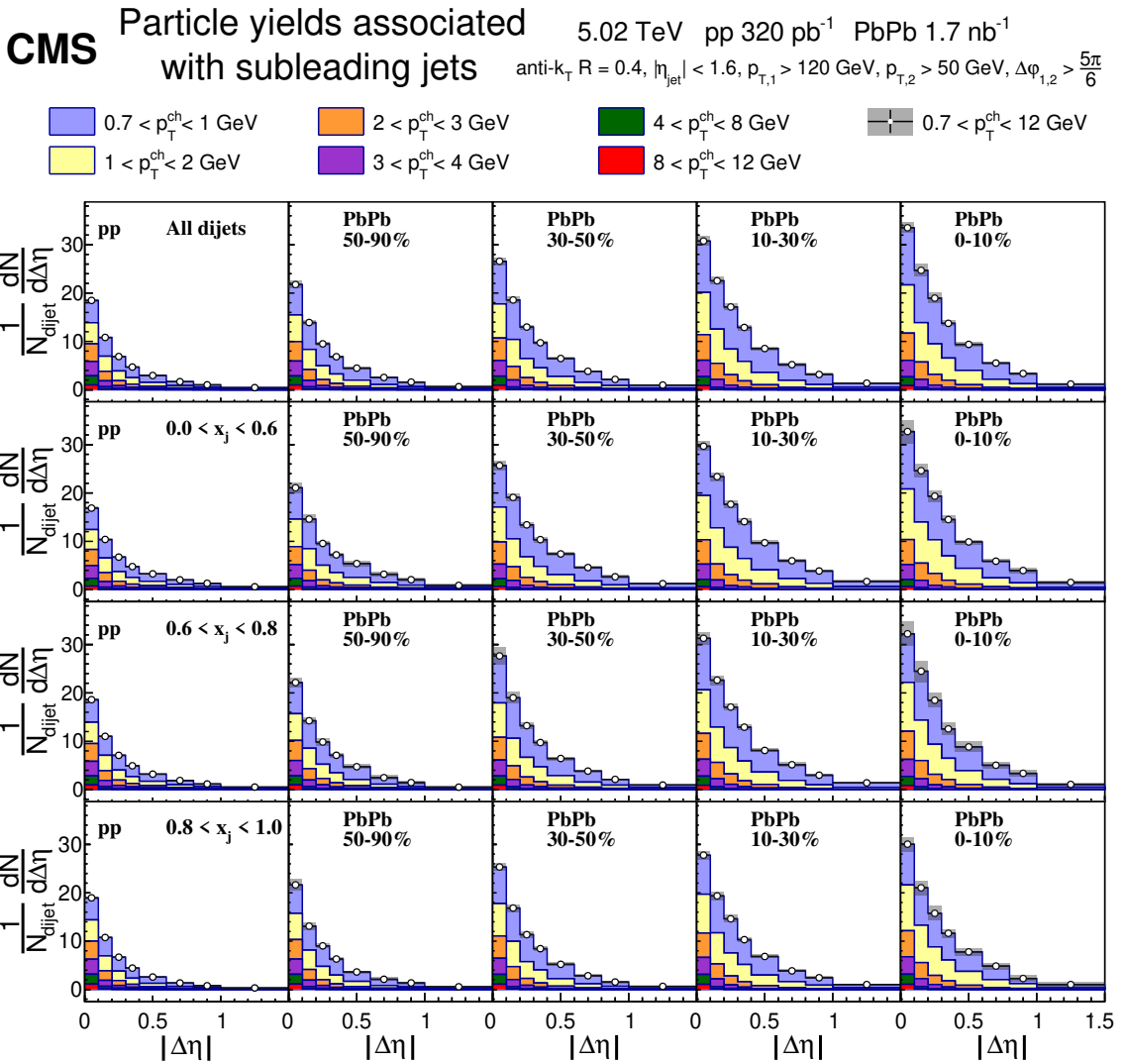


Figure 2. Distributions of charged-particle yields correlated to subleading jets in the region $|\Delta\varphi| < 1$ as a function of $|\Delta\eta|$ for pp (first column) and PbPb (second to fifth columns) collisions in different centrality bins, shown differentially for all p_{T}^{ch} bins. The first row shows the charged-particle yields without any selection on x_j , while other rows show the charged-particle yields in different bins of x_j , starting with the most unbalanced $0 < x_j < 0.6$ (second row) to the most balanced $0.8 < x_j < 1.0$ (fourth row) dijet events.

This does not change significantly as a function of x_j , varying between 3.5% and 3.8% from the most unbalanced to the most balanced studied x_j bins. The other panels are for PbPb collisions in different centrality bins. When compared to pp collisions, there is an enhancement of low- p_{T} charged particles in PbPb collisions. This enhancement is greater for central events than for peripheral events.

The modifications to the leading jet shapes in PbPb collisions are quantified in figure 6, which shows the $\rho(\Delta r)_{\text{PbPb}}/\rho(\Delta r)_{\text{pp}}$ ratios in different centrality and x_j bins. When going toward more central events from the peripheral ones, there is an enhancement of the PbPb

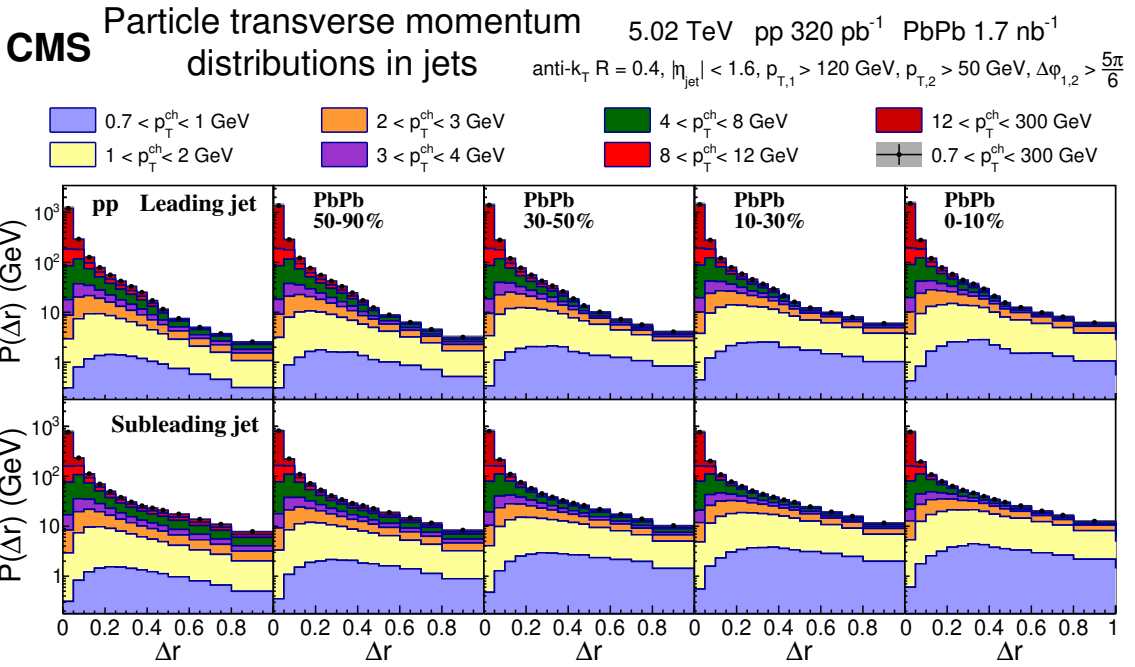


Figure 3. Jet radial momentum profile $P(\Delta r)$ for pp (first column) and PbPb (second to fifth columns) collisions in different centrality bins as a function of Δr , shown differentially in p_T^{ch} for leading (upper row) and subleading (lower row) jets.

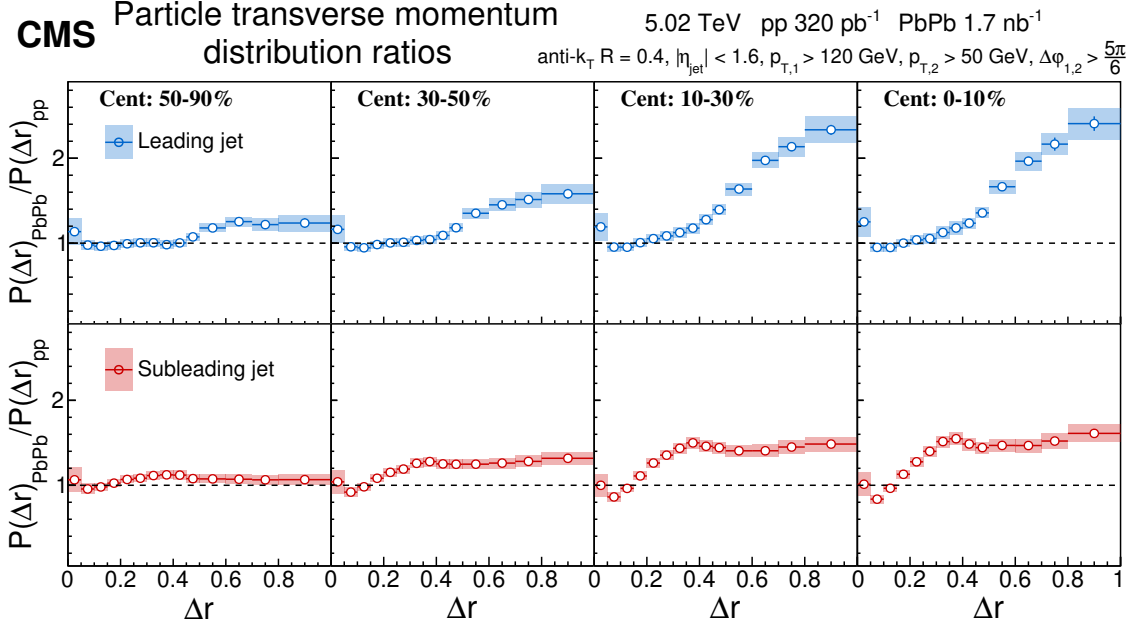


Figure 4. The PbPb to pp ratio of the jet radial momentum distributions as a function of Δr , $P(\Delta r)_{\text{PbPb}}/P(\Delta r)_{\text{pp}}$, for different centrality bins for the leading jets (upper row) and subleading jets (lower row).

CMS Leading jet shape

5.02 TeV pp 320 pb^{-1} PbPb 1.7 nb^{-1}
 $\text{anti-}k_{\text{T}} R = 0.4, |\eta_{\text{jet}}| < 1.6, p_{\text{T},1} > 120 \text{ GeV}, p_{\text{T},2} > 50 \text{ GeV}, \Delta\phi_{1,2} > \frac{5\pi}{6}$

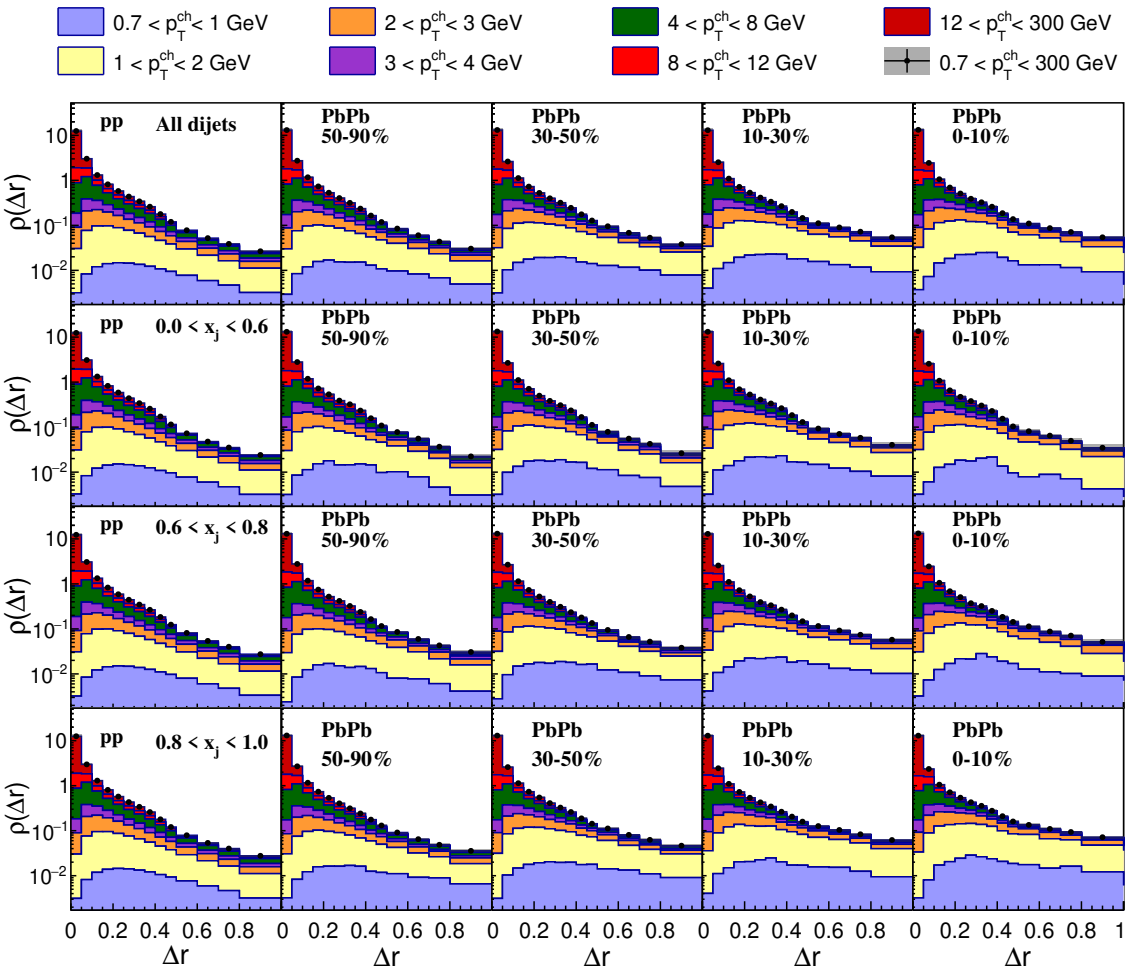


Figure 5. Leading jet shapes $\rho(\Delta r)$ (normalized to unity over $\Delta r < 1$) for pp (first column) and PbPb (second to fifth columns) collisions in different centrality bins as a function of Δr , shown differentially in p_{T}^{ch} for the inclusive x_j bin (first row) and in differential bins $0 < x_j < 0.6$ (second row), $0.6 < x_j < 0.8$ (third row), and $0.8 < x_j < 1.0$ (fourth row).

jet shape compared to the pp shape at large Δr . As already seen in the charged-particle yield plots of figure 1, the differences between pp and PbPb results for leading jets are the largest for the most balanced collisions ($0.8 < x_j < 1.0$) and become smaller as the two jet momenta become less balanced.

Figure 7 shows the jet shape results differentially in charged-particle p_{T} for the sub-leading jets, for different selections of centrality and x_j . As also found for the leading jet results, an enhancement of low- p_{T} charged particles in PbPb collisions is seen for the sub-leading jet. Also, the unbalanced pp collision distribution is not monotonically decreasing toward large Δr , but there is an enhancement around $\Delta r \sim 0.5$, which is mostly caused by high- p_{T} particles. As the jet cone size used for this analysis is $R = 0.4$, these particles

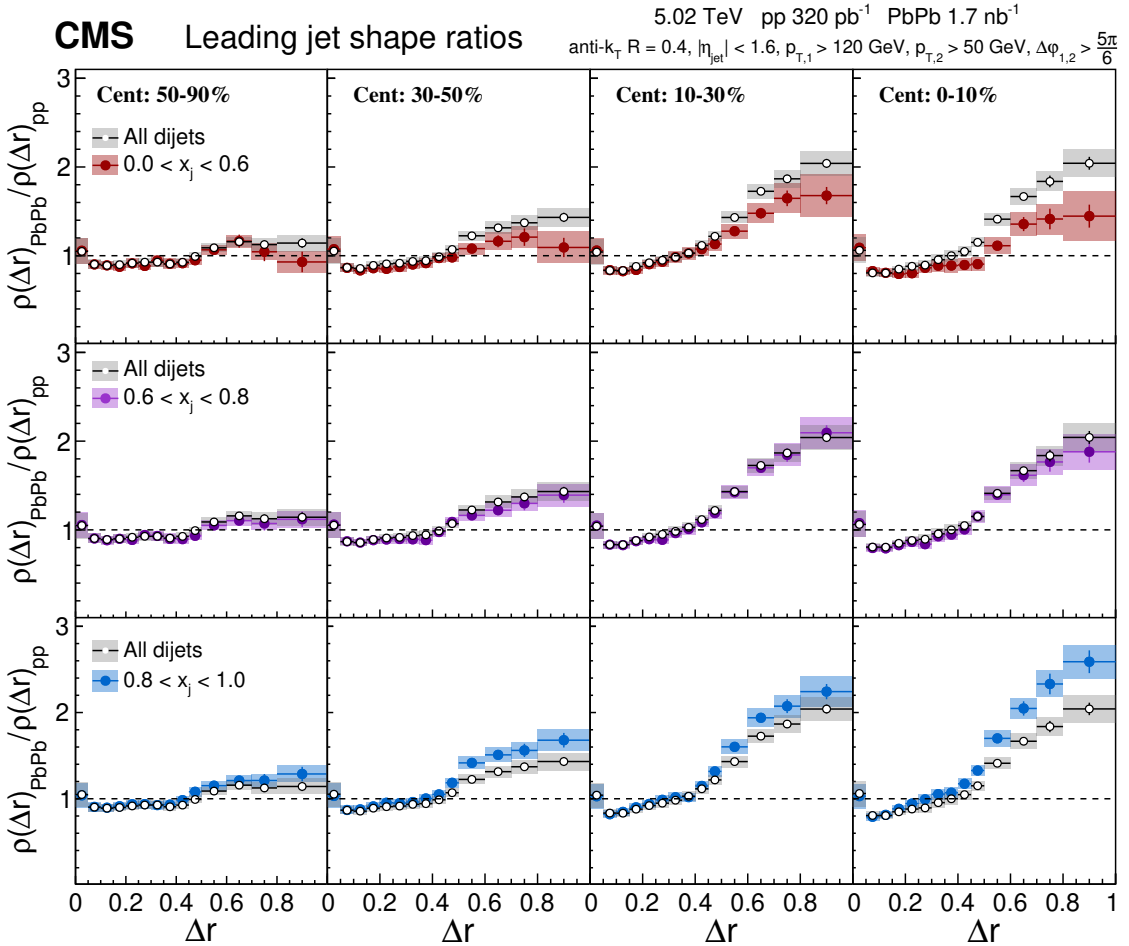


Figure 6. The PbPb to pp ratio as a function of Δr for leading jet shapes, $\rho(\Delta r)_{\text{PbPb}}/\rho(\Delta r)_{\text{pp}}$, in different centrality bins for $0 < x_j < 0.6$ (upper row), $0.6 < x_j < 0.8$ (middle row) and $0.8 < x_j < 1.0$ (lower row) dijet selections. The leading jet shape ratio for all dijets, i.e., without any selection on the dijet momentum balance are also shown in each row for comparison. The error bars represent the statistical uncertainties and the shaded areas the systematic uncertainties.

are not a part of the subleading jet. This enhancement is still somewhat visible in the peripheral PbPb collisions, but disappears for the central events. In the balanced collisions, no enhancement of high- p_T particles at large Δr is visible. To create an unbalanced dijet configuration in pp collisions, there is most often a third jet to conserve momentum, as confirmed by Monte Carlo studies and 3-jet selection in pp events, which explains the enhancement of high- p_T particles outside of the jet cone. The observed features lead to a much more significant x_j dependence for the out-of-cone charged-particle constituent p_T fractions compared to those seen for leading jets. While only 7% of the total charged-particle constituent p_T is out-of-cone for balanced dijets ($0.8 < x_j < 1$) in pp collisions, this fraction increases to 20% for unbalanced dijets ($0 < x_j < 0.6$). Without x_j selection, the fraction is about 11%. In central heavy ion collisions, the jet energy can be lost to the medium and is seen as excess low- p_T particles at larger angles rather than as a third reconstructed jet.

CMS Subleading jet shape

5.02 TeV pp 320 pb^{-1} PbPb 1.7 nb^{-1}
 $\text{anti-}k_{\text{T}} R = 0.4, |\eta_{\text{jet}}| < 1.6, p_{\text{T},1} > 120 \text{ GeV}, p_{\text{T},2} > 50 \text{ GeV}, \Delta\phi_{1,2} > \frac{5\pi}{6}$

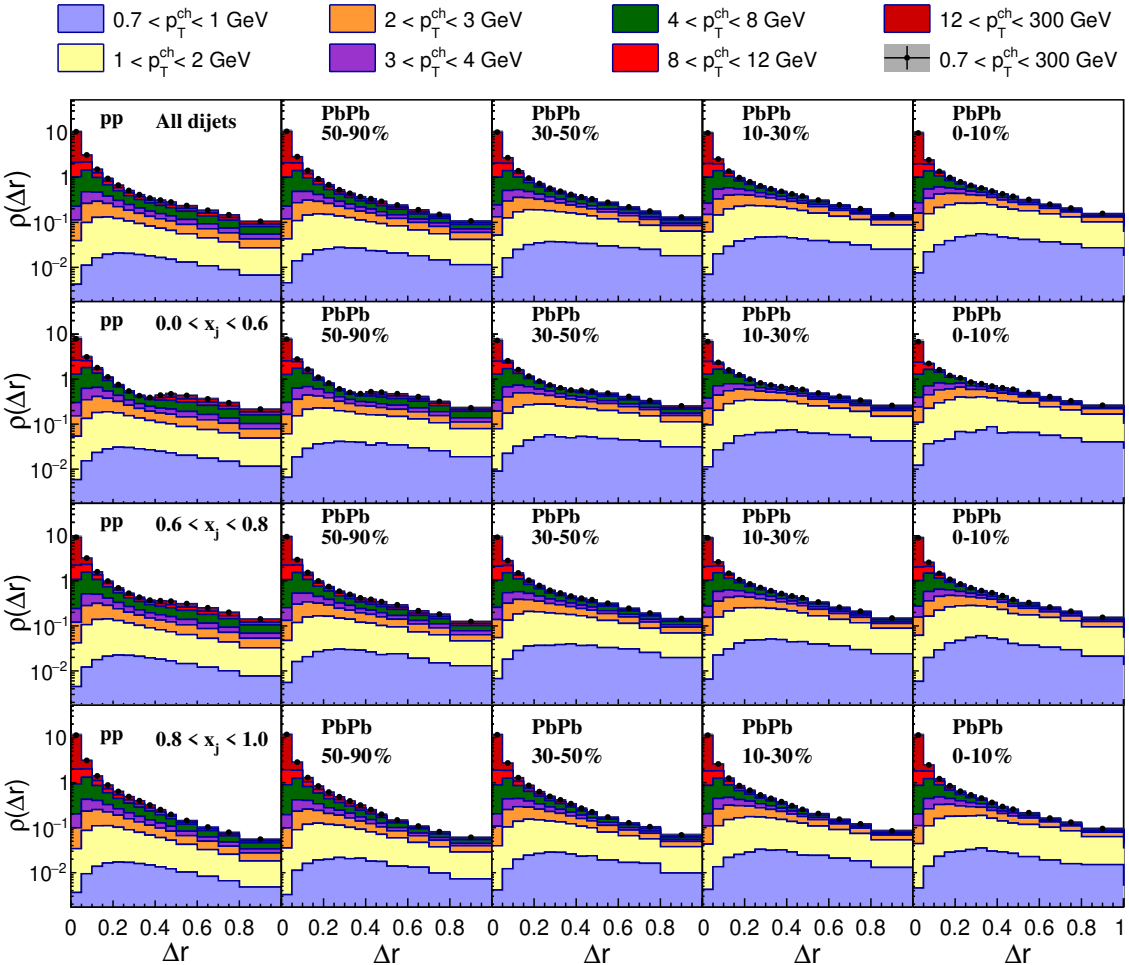


Figure 7. Subleading jet shapes $\rho(\Delta r)$ (normalized to unity over $\Delta r < 1$) for pp (first column) and PbPb (second to fifth columns) collisions in different centrality bins as a function of Δr , shown differentially in p_{T}^{ch} for the inclusive x_j bin (first row) and in differential bins $0 < x_j < 0.6$ (second row), $0.6 < x_j < 0.8$ (third row), and $0.8 < x_j < 1.0$ (fourth row).

The subleading jet shape ratios $\rho(\Delta r)_{\text{PbPb}}/\rho(\Delta r)_{\text{pp}}$ in different centrality and x_j bins are shown in figure 8. There is a broadening of the PbPb jet shape compared to the pp shape when going toward more central events from the peripheral ones. However, in the most unbalanced ($0.0 < x_j < 0.6$) and in moderately balanced ($0.6 < x_j < 0.8$) events, the ratio between PbPb and pp jet shapes first peaks around $\Delta r = 0.4$, then gets close to one at large Δr . The enhancement from small Δr toward the edge of the jet cone at $\Delta r = 0.4$ is explained by jet quenching. Outside the jet cone, the ratio gets closer to unity because of the reduced influence of any potential third jet in PbPb collisions, as discussed for figure 7. If there would be no contribution from particles related to the third jet in the pp jet shape, the enhancement would be the greatest at high Δr also in these events, as is the case for the

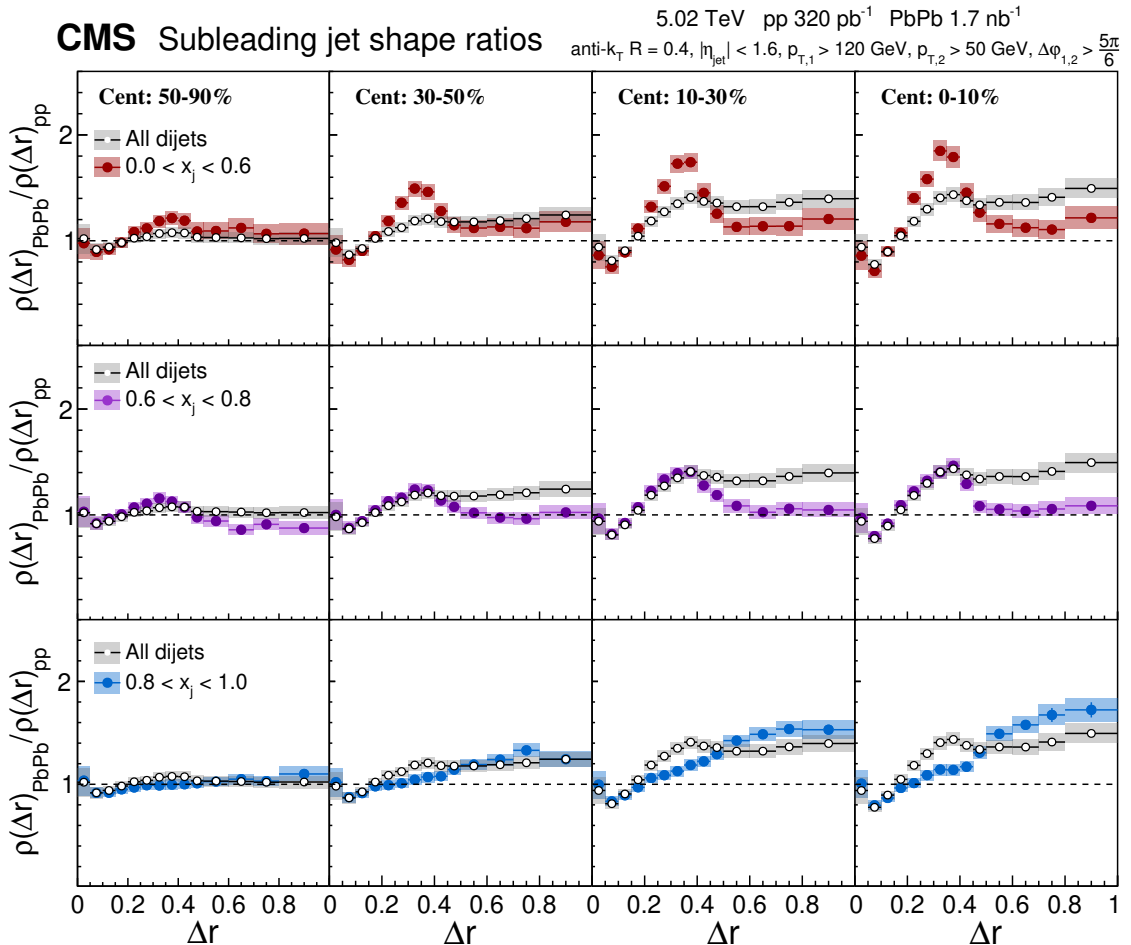


Figure 8. The PbPb to pp ratio as a function of Δr for subleading jet shapes, $\rho(\Delta r)_{\text{PbPb}}/\rho(\Delta r)_{\text{pp}}$, in different centrality bins for $0 < x_j < 0.6$ (upper row), $0.6 < x_j < 0.8$ (middle row) and $0.8 < x_j < 1.0$ (lower row) dijet selections. The subleading jet shape ratio for all dijets, i.e., without any selection on the dijet momentum balance are also shown in each row for comparison. The error bars represent the statistical uncertainties and the shaded areas the systematic uncertainties.

most balanced ($0.8 < x_j < 1.0$) events. Notice that the leading and subleading jet p_T can still be up to 20% different in this most balanced bin. This explains the ratio differences in this bin between leading jets in figure 6 and subleading jets in figure 8.

The ratio of jet shapes in momentum balanced and unbalanced samples with the x_j inclusive sample for leading jets is presented in figure 9 and for subleading jets in figure 10. Taking this ratio cancels the systematic uncertainties related to tracking and the jet energy scale. However, the uncertainties related to the jet energy resolution do not cancel and are included in the systematic uncertainties. For the leading jets, the jet shapes in the unbalanced $0 < x_j < 0.6$ bin are narrower than in the x_j inclusive sample. Conversely, in the balanced $0.8 < x_j < 1.0$ bin, the jet shapes are wider. For the subleading jets in figure 10, the behavior is exactly opposite to the leading jets, the jet shapes in the unbalanced bin are wider and in the balanced bin narrower compared to the x_j inclusive case. This is similar to the x_j dependence seen for the charged-particle distributions.

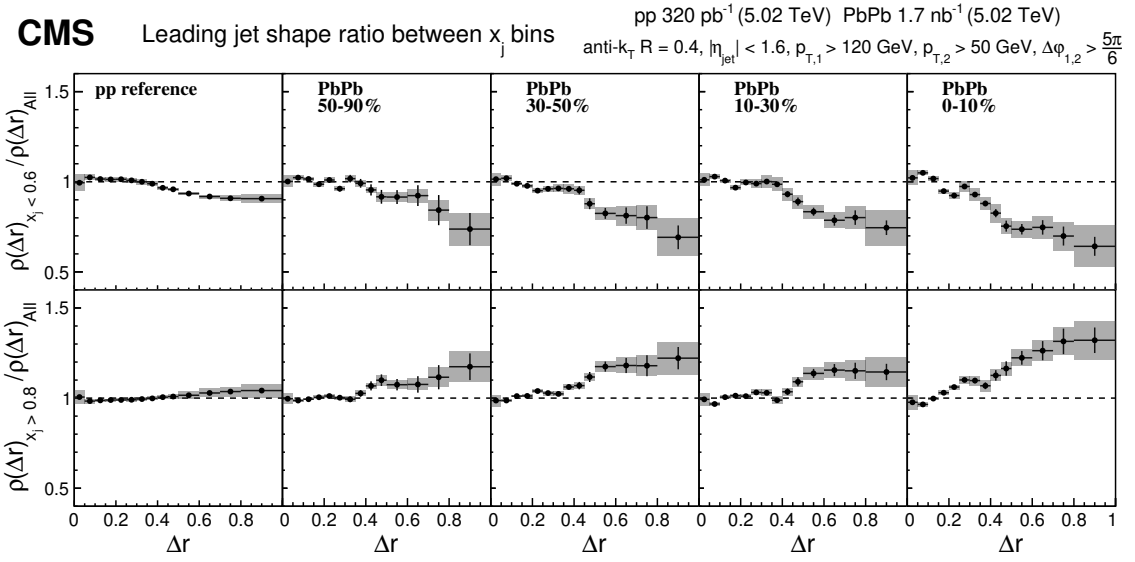


Figure 9. Ratio of momentum-unbalanced ($0.0 < x_j < 0.6$, upper row) and balanced ($0.8 < x_j < 1.0$, lower row) jet shapes to x_j integrated jet shapes for leading jets in pp collisions and different PbPb centrality bins as a function of Δr . The error bars represent the statistical uncertainties and the shaded areas the systematic uncertainties.

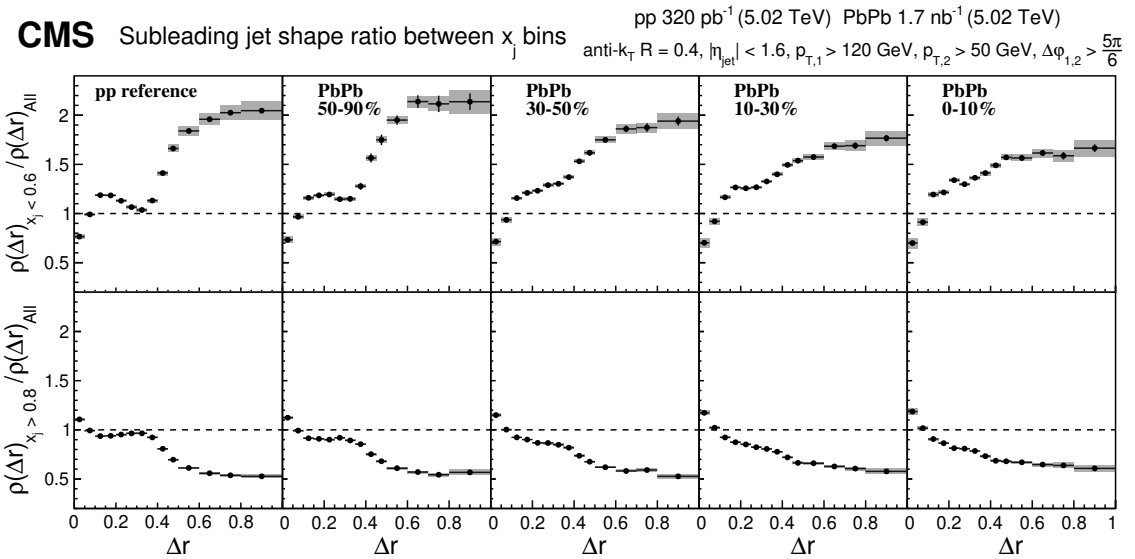


Figure 10. Ratio of momentum-unbalanced ($0.0 < x_j < 0.6$, upper row) and balanced ($0.8 < x_j < 1.0$, lower row) jet shapes to x_j integrated jet shapes for subleading jets in pp collisions and different PbPb centrality bins as a function of Δr . The error bars represent the statistical uncertainties and the shaded areas the systematic uncertainties.

8 Summary

The CMS experiment has measured charged-particle yields and jet shapes in events containing back-to-back dijet pairs around the jet axes using data from proton-proton (pp) and lead-lead (PbPb) collisions at $\sqrt{s_{\text{NN}}} = 5.02 \text{ TeV}$ collected in 2017 and 2018. When comparing the charged-particle yields around the jet axes, an excess of low transverse momentum (p_T) particles is observed in PbPb with respect to pp collisions. This excess is larger for subleading jets compared to leading jets. The excess is also found to have a different dijet momentum balance $x_j = p_T^{\text{subleading}}/p_T^{\text{leading}}$ dependence for the leading and subleading jets. A possible cause for x_j imbalance is that the leading jet is produced near the surface of the quark-gluon plasma while the subleading jet needs to traverse a longer distance through the plasma. The leading jets show the strongest modifications in balanced events ($x_j \approx 1$), while subleading jets experience the most pronounced modifications in events with a large jet momentum imbalance. A possible explanation is that in balanced events both jets lose a comparable amount of energy, while in events with a momentum imbalance the leading jet loses significantly less energy. Furthermore, jet quenching could lead to the reversal of the apparent leading/subleading ordering and energy loss fluctuations in PbPb collisions could also play a role.

For the jet shapes, which are normalized distributions of charged-particle transverse momentum as a function of the distance from the jet axis, a redistribution of energy is observed from small angles with respect to the jet axis to larger angles when comparing PbPb and pp events. The difference between the PbPb and pp results is larger for the leading jets compared to the subleading jets, which can be explained by the subleading jet distribution in pp collisions being significantly wider than that for leading jets. When studying the unbalanced x_j selection for the subleading jets in pp collisions, a fragmentation pattern consistent with the presence of a third jet is observed. Such a pattern is not observed in balanced pp events or in the PbPb sample. As a result, the enhancement of the PbPb to pp ratio for unbalanced events peaks around $\Delta r = 0.4$ and becomes smaller at larger Δr .

When comparing the jet shapes corresponding to different dijet momentum balance conditions, the distributions for leading jets are found to be the widest for events with balanced jet momenta. For subleading jets, the situation is the opposite, and the widest distributions are found from events having a significant momentum imbalance. These observations are consistent with the interpretation of the charged-particle yield measurements, namely that the average path length inside the medium for leading jets is larger for momentum balanced events, while for subleading jets it is larger in unbalanced events. By studying the charged-particle yields correlated to jets and jet shapes for the first time as a function of dijet momentum balance, this study provides new constraints to the theoretical models and provides a unique way to explore the transition between the domains of weakly and strongly interacting QCD matter.

Acknowledgments

We congratulate our colleagues in the CERN accelerator departments for the excellent performance of the LHC and thank the technical and administrative staffs at CERN and at other CMS institutes for their contributions to the success of the CMS effort. In addition, we gratefully acknowledge the computing centres and personnel of the Worldwide

LHC Computing Grid and other centres for delivering so effectively the computing infrastructure essential to our analyses. Finally, we acknowledge the enduring support for the construction and operation of the LHC, the CMS detector, and the supporting computing infrastructure provided by the following funding agencies: BMBWF and FWF (Austria); FNRS and FWO (Belgium); CNPq, CAPES, FAPERJ, FAPERGS, and FAPESP (Brazil); MES (Bulgaria); CERN; CAS, MoST, and NSFC (China); COLCIENCIAS (Colombia); MSES and CSF (Croatia); RIF (Cyprus); SENESCYT (Ecuador); MoER, ERC PUT and ERDF (Estonia); Academy of Finland, MEC, and HIP (Finland); CEA and CNRS/IN2P3 (France); BMBF, DFG, and HGF (Germany); GSRT (Greece); NKFIA (Hungary); DAE and DST (India); IPM (Iran); SFI (Ireland); INFN (Italy); MSIP and NRF (Republic of Korea); MES (Latvia); LAS (Lithuania); MOE and UM (Malaysia); BUAP, CINVESTAV, CONACYT, LNS, SEP, and UASLP-FAI (Mexico); MOS (Montenegro); MBIE (New Zealand); PAEC (Pakistan); MSHE and NSC (Poland); FCT (Portugal); JINR (Dubna); MON, RosAtom, RAS, RFBR, and NRC KI (Russia); MESTD (Serbia); SEIDI, CPAN, PCTI, and FEDER (Spain); MOSTR (Sri Lanka); Swiss Funding Agencies (Switzerland); MST (Taipei); The EP Center, IPST, STAR, and NSTDA (Thailand); TUBITAK and TAEK (Turkey); NASU (Ukraine); STFC (United Kingdom); DOE and NSF (U.S.A.).

Individuals have received support from the Marie-Curie programme and the European Research Council and Horizon 2020 Grant, contract Nos. 675440, 724704, 752730, and 765710 (European Union); the Leventis Foundation; the Alfred P. Sloan Foundation; the Alexander von Humboldt Foundation; the Belgian Federal Science Policy Office; the Fonds pour la Formation à la Recherche dans l’Industrie et dans l’Agriculture (FRIA-Belgium); the Agentschap voor Innovatie door Wetenschap en Technologie (IWT-Belgium); the F.R.S.-FNRS and FWO (Belgium) under the “Excellence of Science – EOS” – be.h project n. 30820817; the Beijing Municipal Science & Technology Commission, No. Z191100007219010; the Ministry of Education, Youth and Sports (MEYS) of the Czech Republic; the Deutsche Forschungsgemeinschaft (DFG), under Germany’s Excellence Strategy – EXC 2121 “Quantum Universe” – 390833306, and under project number 400140256 – GRK2497; the Lendület (“Momentum”) Programme and the János Bolyai Research Scholarship of the Hungarian Academy of Sciences, the New National Excellence Program ÚNKP, the NKFIA research grants 123842, 123959, 124845, 124850, 125105, 128713, 128786, and 129058 (Hungary); the Council of Science and Industrial Research, India; the HOMING PLUS programme of the Foundation for Polish Science, cofinanced from European Union, Regional Development Fund, the Mobility Plus programme of the Ministry of Science and Higher Education, the National Science Center (Poland), contracts Harmonia 2014/14/M/ST2/00428, Opus 2014/13/B/ST2/02543, 2014/15/B/ST2/03998, and 2015/19/B/ST2/02861, Sonata-bis 2012/07/E/ST2/01406; the National Priorities Research Program by Qatar National Research Fund; the Ministry of Science and Higher Education, project no. 0723-2020-0041 (Russia); the Tomsk Polytechnic University Competitiveness Enhancement Program; the Programa Estatal de Fomento de la Investigación Científica y Técnica de Excelencia María de Maeztu, grant MDM-2015-0509 and the Programa Severo Ochoa del Principado de Asturias; the Thalis and Aristeia programmes cofinanced by EU-ESF and the Greek NSRF; the Rachadapisek Sompot Fund for Postdoctoral Fellowship, Chulalongkorn University and the Chulalongkorn Academic into Its 2nd Century Project Advancement Project (Thailand); the Kavli Foundation; the Nvidia Corporation; the SuperMicro Corporation; the Welch Foundation, contract C-1845; and the Weston Havens Foundation (U.S.A.).

A Dijet momentum balance migration matrices

Jet energy resolution effects may cause the x_j of the dijet system to migrate from one bin to another. The magnitude of this effect can be estimated from simulation. The plots illustrating x_j bin migrations in PYTHIA 8 (pp) and PYTHIA+HYDJET (PbPb) simulations are presented in figures 11 and 12. The plots in figure 11 give the probability for the generator level dijet to be in a specific x_j bin, given the x_j bin for the reconstructed dijet while those in figure 12 give the probability for the reconstructed dijet to be in a specific x_j bin, given the x_j bin for the generator level dijet. For example, for the PYTHIA 8 simulation in the leftmost plot of the top row in figure 11, if the reconstructed dijet is in the bin $0 < x_j < 0.6$, the probability that the generator level dijet is also in this bin is 56.5%. It can be seen from these plots that the x_j values in central heavy collisions are more strongly broadened than in pp collisions in the simulation. In general, generator-level x_j values tend to be higher than the reconstructed ones, meaning that jet energy resolution effects cause dijets to be more unbalanced.

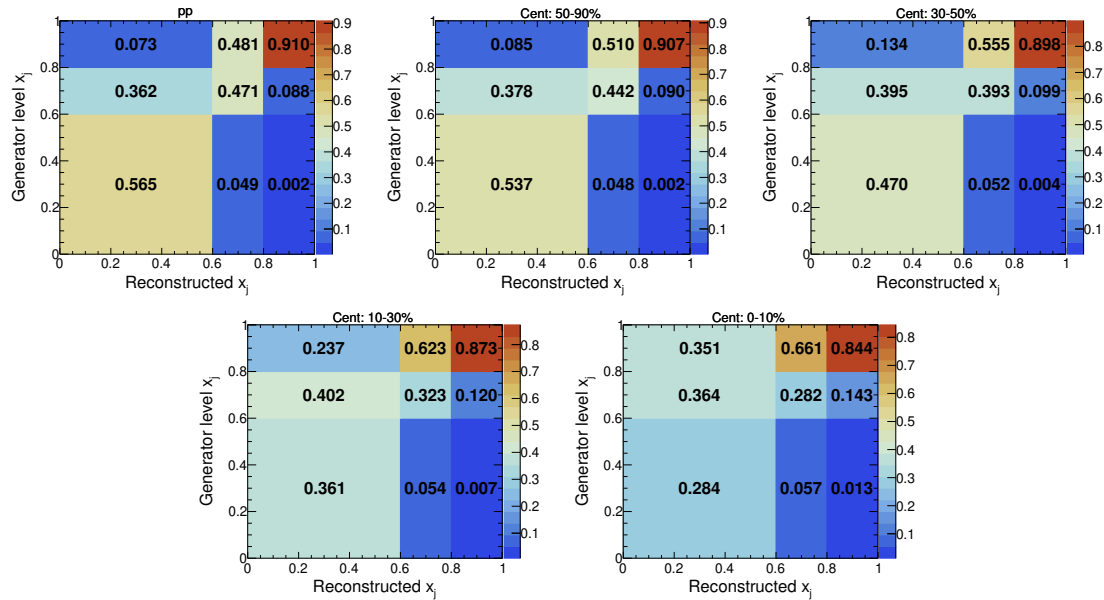


Figure 11. Generator-level vs. reconstructed x_j values in the analysis x_j bins. The plots show the probability to find a generator level x_j for a given reconstructed x_j . The PYTHIA 8 simulation is shown in the upper-left plot while the most central PYTHIA+HYDJET is shown in the lower-right plot.

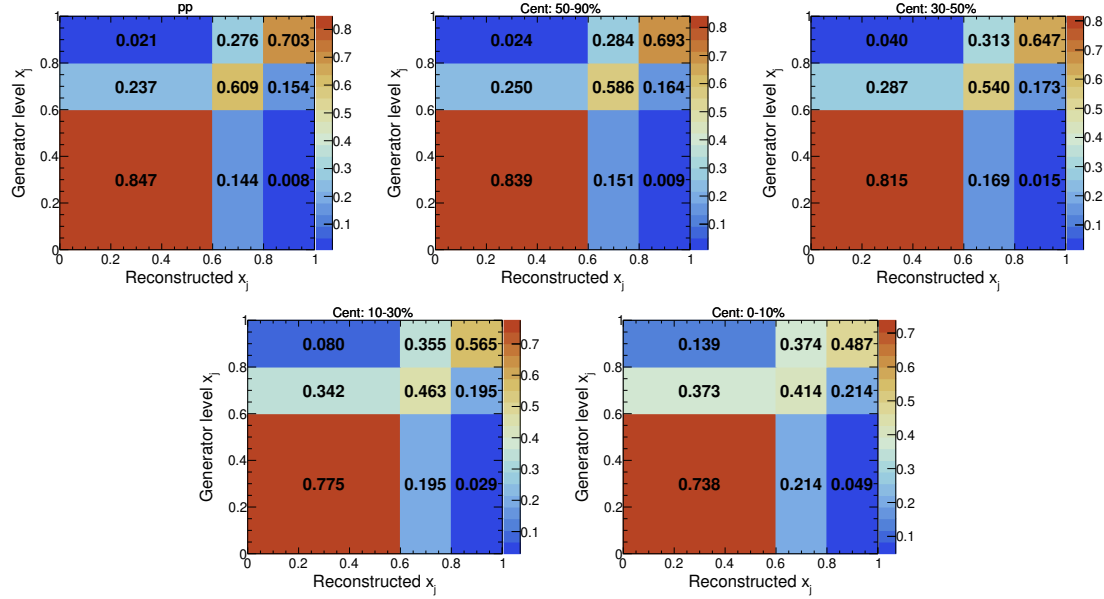


Figure 12. Generator-level vs. reconstructed x_j values in the analysis x_j bins. The plots show the probability to find a reconstructed x_j for a given generator level x_j . The PYTHIA 8 simulation is shown in the upper-left plot while the most central PYTHIA+HYDJET is shown in the lower-right plot.

Open Access. This article is distributed under the terms of the Creative Commons Attribution License ([CC-BY 4.0](#)), which permits any use, distribution and reproduction in any medium, provided the original author(s) and source are credited.

References

- [1] W. Busza, K. Rajagopal and W. van der Schee, *Heavy ion collisions: the big picture, and the big questions*, *Ann. Rev. Nucl. Part. Sci.* **68** (2018) 339 [[arXiv:1802.04801](#)] [[INSPIRE](#)].
- [2] J.D. Bjorken, *Energy loss of energetic partons in QGP: possible extinction of high p_T jets in hadron-hadron collisions*, [FERMILAB-PUB-82-059-THY](#) (1982).
- [3] STAR collaboration, *Direct observation of dijets in central Au+Au collisions at $\sqrt{s_{\text{NN}}} = 200 \text{ GeV}$* , *Phys. Rev. Lett.* **97** (2006) 162301 [[nucl-ex/0604018](#)] [[INSPIRE](#)].
- [4] PHENIX collaboration, *Transverse momentum and centrality dependence of dihadron correlations in Au+Au collisions at $\sqrt{s_{\text{NN}}} = 200 \text{ GeV}$: Jet-quenching and the response of partonic matter*, *Phys. Rev. C* **77** (2008) 011901 [[arXiv:0705.3238](#)] [[INSPIRE](#)].
- [5] ATLAS collaboration, *Observation of a centrality-dependent dijet asymmetry in lead-lead collisions at $\sqrt{s_{\text{NN}}} = 2.76 \text{ TeV}$ with the ATLAS detector at the LHC*, *Phys. Rev. Lett.* **105** (2010) 252303 [[arXiv:1011.6182](#)] [[INSPIRE](#)].
- [6] CMS collaboration, *Observation and studies of jet quenching in PbPb collisions at $\sqrt{s_{\text{NN}}} = 2.76 \text{ TeV}$* , *Phys. Rev. C* **84** (2011) 024906 [[arXiv:1102.1957](#)] [[INSPIRE](#)].
- [7] CMS collaboration, *Jet momentum dependence of jet quenching in PbPb collisions at $\sqrt{s_{\text{NN}}} = 2.76 \text{ TeV}$* , *Phys. Lett. B* **712** (2012) 176 [[arXiv:1202.5022](#)] [[INSPIRE](#)].
- [8] ALICE collaboration, *Measurement of jet suppression in central Pb–Pb collisions at $\sqrt{s_{\text{NN}}} = 2.76 \text{ TeV}$* , *Phys. Lett. B* **746** (2015) 1 [[arXiv:1502.01689](#)] [[INSPIRE](#)].

- [9] BRAHMS collaboration, *Quark gluon plasma and color glass condensate at RHIC? The Perspective from the BRAHMS experiment*, *Nucl. Phys. A* **757** (2005) 1 [[nucl-ex/0410020](#)] [[INSPIRE](#)].
- [10] PHOBOS collaboration, *The PHOBOS perspective on discoveries at RHIC*, *Nucl. Phys. A* **757** (2005) 28 [[nucl-ex/0410022](#)] [[INSPIRE](#)].
- [11] STAR collaboration, *Experimental and theoretical challenges in the search for the quark gluon plasma: The STAR Collaboration’s critical assessment of the evidence from RHIC collisions*, *Nucl. Phys. A* **757** (2005) 102 [[nucl-ex/0501009](#)] [[INSPIRE](#)].
- [12] PHENIX collaboration, *Formation of dense partonic matter in relativistic nucleus-nucleus collisions at RHIC: Experimental evaluation by the PHENIX collaboration*, *Nucl. Phys. A* **757** (2005) 184 [[nucl-ex/0410003](#)] [[INSPIRE](#)].
- [13] CMS collaboration, *Measurement of jet fragmentation in PbPb and pp collisions at $\sqrt{s_{\text{NN}}} = 2.76 \text{ TeV}$* , *Phys. Rev. C* **90** (2014) 024908 [[arXiv:1406.0932](#)] [[INSPIRE](#)].
- [14] ATLAS collaboration, *Measurement of inclusive jet charged-particle fragmentation functions in Pb+Pb collisions at $\sqrt{s_{\text{NN}}} = 2.76 \text{ TeV}$ with the ATLAS detector*, *Phys. Lett. B* **739** (2014) 320 [[arXiv:1406.2979](#)] [[INSPIRE](#)].
- [15] CMS collaboration, *Modification of jet shapes in PbPb collisions at $\sqrt{s_{\text{NN}}} = 2.76 \text{ TeV}$* , *Phys. Lett. B* **730** (2014) 243 [[arXiv:1310.0878](#)] [[INSPIRE](#)].
- [16] CMS collaboration, *Measurement of transverse momentum relative to dijet systems in PbPb and pp collisions at $\sqrt{s_{\text{NN}}} = 2.76 \text{ TeV}$* , *JHEP* **01** (2016) 006 [[arXiv:1509.09029](#)] [[INSPIRE](#)].
- [17] CMS collaboration, *Correlations between jets and charged particles in PbPb and pp collisions at $\sqrt{s_{\text{NN}}} = 2.76 \text{ TeV}$* , *JHEP* **02** (2016) 156 [[arXiv:1601.00079](#)] [[INSPIRE](#)].
- [18] CMS collaboration, *Decomposing transverse momentum balance contributions for quenched jets in PbPb collisions at $\sqrt{s_{\text{NN}}} = 2.76 \text{ TeV}$* , *JHEP* **11** (2016) 055 [[arXiv:1609.02466](#)] [[INSPIRE](#)].
- [19] CMS collaboration, *Jet properties in PbPb and pp collisions at $\sqrt{s_{\text{NN}}} = 5.02 \text{ TeV}$* , *JHEP* **05** (2018) 006 [[arXiv:1803.00042](#)] [[INSPIRE](#)].
- [20] L. Apolinario, N. Armesto and L. Cunqueiro, *An analysis of the influence of background subtraction and quenching on jet observables in heavy-ion collisions*, *JHEP* **02** (2013) 022 [[arXiv:1211.1161](#)] [[INSPIRE](#)].
- [21] A. Ayala, I. Dominguez, J. Jalilian-Marian and M.E. Tejeda-Yeomans, *Jet asymmetry and momentum imbalance from $2 \rightarrow 2$ and $2 \rightarrow 3$ partonic processes in relativistic heavy-ion collisions*, *Phys. Rev. C* **92** (2015) 044902 [[arXiv:1503.06889](#)] [[INSPIRE](#)].
- [22] J.-P. Blaizot, Y. Mehtar-Tani and M.A.C. Torres, *Angular structure of the in-medium QCD cascade*, *Phys. Rev. Lett.* **114** (2015) 222002 [[arXiv:1407.0326](#)] [[INSPIRE](#)].
- [23] M.A. Escobedo and E. Iancu, *Event-by-event fluctuations in the medium-induced jet evolution*, *JHEP* **05** (2016) 008 [[arXiv:1601.03629](#)] [[INSPIRE](#)].
- [24] J. Casalderrey-Solana, D. Gulhan, G. Milhano, D. Pablos and K. Rajagopal, *Angular structure of jet quenching within a hybrid strong/weak coupling model*, *JHEP* **03** (2017) 135 [[arXiv:1609.05842](#)] [[INSPIRE](#)].
- [25] Y. Tachibana, N.-B. Chang and G.-Y. Qin, *Full jet in quark-gluon plasma with hydrodynamic medium response*, *Phys. Rev. C* **95** (2017) 044909 [[arXiv:1701.07951](#)] [[INSPIRE](#)].
- [26] CMS collaboration, *Performance of the CMS level-1 trigger in proton-proton collisions at $\sqrt{s} = 13 \text{ TeV}$, 2020* *JINST* **15** P10017 [[arXiv:2006.10165](#)] [[INSPIRE](#)].
- [27] CMS collaboration, *The CMS trigger system, 2017* *JINST* **12** P01020 [[arXiv:1609.02366](#)] [[INSPIRE](#)].

- [28] CMS collaboration, *The CMS Experiment at the CERN LHC*, **2008 JINST** **3** S08004 [[INSPIRE](#)].
- [29] M. Cacciari, G.P. Salam and G. Soyez, *The anti- k_T jet clustering algorithm*, **JHEP** **04** (2008) 063 [[arXiv:0802.1189](#)] [[INSPIRE](#)].
- [30] O. Kodolova, I. Vardanyan, A. Nikitenko and A. Oulianov, *The performance of the jet identification and reconstruction in heavy ions collisions with CMS detector*, **Eur. Phys. J. C** **50** (2007) 117 [[INSPIRE](#)].
- [31] CMS collaboration, *Dependence on pseudorapidity and centrality of charged hadron production in PbPb collisions at a nucleon-nucleon centre-of-mass energy of 2.76 TeV*, **JHEP** **08** (2011) 141 [[arXiv:1107.4800](#)] [[INSPIRE](#)].
- [32] T. Sjöstrand et al., *An introduction to PYTHIA 8.2*, **Comput. Phys. Commun.** **191** (2015) 159 [[arXiv:1410.3012](#)] [[INSPIRE](#)].
- [33] CMS collaboration, *Extraction and validation of a new set of CMS PYTHIA8 tunes from underlying-event measurements*, **Eur. Phys. J. C** **80** (2020) 4 [[arXiv:1903.12179](#)] [[INSPIRE](#)].
- [34] NNPDF collaboration, *Parton distributions from high-precision collider data*, **Eur. Phys. J. C** **77** (2017) 663 [[arXiv:1706.00428](#)] [[INSPIRE](#)].
- [35] GEANT4 collaboration, *GEANT4 — a simulation toolkit*, **Nucl. Instrum. Meth. A** **506** (2003) 250 [[INSPIRE](#)].
- [36] I.P. Lokhtin, L.V. Malinina, S.V. Petrushanko, A.M. Snigirev, I. Arsene and K. Tywoniuk, *Heavy ion event generator HYDJET++ (HYDrodynamics plus JETs)*, **Comput. Phys. Commun.** **180** (2009) 779 [[arXiv:0809.2708](#)] [[INSPIRE](#)].
- [37] M. Cacciari, G.P. Salam and G. Soyez, *FastJet User Manual*, **Eur. Phys. J. C** **72** (2012) 1896 [[arXiv:1111.6097](#)] [[INSPIRE](#)].
- [38] CMS collaboration, *Particle-flow reconstruction and global event description with the CMS detector*, **2017 JINST** **12** P10003 [[arXiv:1706.04965](#)] [[INSPIRE](#)].
- [39] D. Bertolini, T. Chan and J. Thaler, *Jet observables without jet algorithms*, **JHEP** **04** (2014) 013 [[arXiv:1310.7584](#)] [[INSPIRE](#)].
- [40] A.J. Larkoski, D. Neill and J. Thaler, *Jet shapes with the broadening axis*, **JHEP** **04** (2014) 017 [[arXiv:1401.2158](#)] [[INSPIRE](#)].
- [41] P. Berta, M. Spousta, D.W. Miller and R. Leitner, *Particle-level pileup subtraction for jets and jet shapes*, **JHEP** **06** (2014) 092 [[arXiv:1403.3108](#)] [[INSPIRE](#)].
- [42] CMS collaboration, *Description and performance of track and primary-vertex reconstruction with the CMS tracker*, **2014 JINST** **9** P10009 [[arXiv:1405.6569](#)] [[INSPIRE](#)].
- [43] CMS collaboration, *Charged-particle nuclear modification factors in PbPb and pPb collisions at $\sqrt{s_{\text{NN}}} = 5.02 \text{ TeV}$* , **JHEP** **04** (2017) 039 [[arXiv:1611.01664](#)] [[INSPIRE](#)].
- [44] CMS collaboration, *Measurement of jet fragmentation into charged particles in pp and PbPb collisions at $\sqrt{s_{\text{NN}}} = 2.76 \text{ TeV}$* , **JHEP** **10** (2012) 087 [[arXiv:1205.5872](#)] [[INSPIRE](#)].
- [45] CMS collaboration, *Jet energy scale and resolution in the CMS experiment in pp collisions at 8 TeV*, **2017 JINST** **12** P02014 [[arXiv:1607.03663](#)] [[INSPIRE](#)].
- [46] T. Renk, *Theoretical assessment of jet-hadron correlations*, **Phys. Rev. C** **87** (2013) 024905 [[arXiv:1210.1330](#)] [[INSPIRE](#)].
- [47] J.G. Milhano and K.C. Zapp, *Origins of the di-jet asymmetry in heavy ion collisions*, **Eur. Phys. J. C** **76** (2016) 288 [[arXiv:1512.08107](#)] [[INSPIRE](#)].

The CMS collaboration

Yerevan Physics Institute, Yerevan, Armenia

A.M. Sirunyan[†], A. Tumasyan

Institut für Hochenergiephysik, Wien, Austria

W. Adam, T. Bergauer, M. Dragicevic, J. Erö, A. Escalante Del Valle, R. Frühwirth¹, M. Jeitler¹, N. Krammer, L. Lechner, D. Liko, T. Madlener, I. Mikulec, F.M. Pitters, N. Rad, J. Schieck¹, R. Schöfbeck, M. Spanring, S. Templ, W. Waltenberger, C.-E. Wulz¹, M. Zarucki

Institute for Nuclear Problems, Minsk, Belarus

V. Chekhovsky, A. Litomin, V. Makarenko, J. Suarez Gonzalez

Universiteit Antwerpen, Antwerpen, Belgium

M.R. Darwish², E.A. De Wolf, D. Di Croce, X. Janssen, T. Kello³, A. Lelek, M. Pieters, H. Rejeb Sfar, H. Van Haevermaet, P. Van Mechelen, S. Van Putte, N. Van Remortel

Vrije Universiteit Brussel, Brussel, Belgium

F. Blekman, E.S. Bols, S.S. Chhibra, J. D'Hondt, J. De Clercq, D. Lontkovskyi, S. Lowette, I. Marchesini, S. Moortgat, A. Morton, Q. Python, S. Tavernier, W. Van Doninck, P. Van Mulders

Université Libre de Bruxelles, Bruxelles, Belgium

D. Beghin, B. Bilin, B. Clerbaux, G. De Lentdecker, B. Dorney, L. Favart, A. Grebenyuk, A.K. Kalsi, I. Makarenko, L. Moureaux, L. Pétré, A. Popov, N. Postiau, E. Starling, L. Thomas, C. Vander Velde, P. Vanlaer, D. Vannerom, L. Wezenbeek

Ghent University, Ghent, Belgium

T. Cornelis, D. Dobur, M. Gruchala, I. Khvastunov⁴, M. Niedziela, C. Roskas, K. Skovpen, M. Tytgat, W. Verbeke, B. Vermassen, M. Vit

Université Catholique de Louvain, Louvain-la-Neuve, Belgium

G. Bruno, F. Bury, C. Caputo, P. David, C. Delaere, M. Delcourt, I.S. Donertas, A. Giannanco, V. Lemaitre, K. Mondal, J. Prisciandaro, A. Taliercio, M. Teklishyn, P. Vischia, S. Wertz, S. Wuyckens

Centro Brasileiro de Pesquisas Físicas, Rio de Janeiro, Brazil

G.A. Alves, C. Hensel, A. Moraes

Universidade do Estado do Rio de Janeiro, Rio de Janeiro, Brazil

W.L. Aldá Júnior, E. Belchior Batista Das Chagas, H. Brandao Malbouisson, W. Carvalho, J. Chinellato⁵, E. Coelho, E.M. Da Costa, G.G. Da Silveira⁶, D. De Jesus Damiao, S. Fonseca De Souza, J. Martins⁷, D. Matos Figueiredo, M. Medina Jaime⁸, C. Mora Herrera, L. Mundim, H. Nogima, P. Rebello Teles, L.J. Sanchez Rosas, A. Santoro, S.M. Silva Do Amaral, A. Sznajder, M. Thiel, F. Torres Da Silva De Araujo, A. Vilela Pereira

Universidade Estadual Paulista ^a, Universidade Federal do ABC ^b, São Paulo, Brazil

C.A. Bernardes^a, L. Calligaris^a, T.R. Fernandez Perez Tomei^a, E.M. Gregores^{a,b}, D.S. Lemos^a, P.G. Mercadante^{a,b}, S.F. Novaes^a, Sandra S. Padula^a

Institute for Nuclear Research and Nuclear Energy, Bulgarian Academy of Sciences, Sofia, Bulgaria

A. Aleksandrov, G. Antchev, I. Atanasov, R. Hadjiiska, P. Iaydjiev, M. Misheva, M. Rodozov, M. Shopova, G. Sultanov

University of Sofia, Sofia, Bulgaria

M. Bonchev, A. Dimitrov, T. Ivanov, L. Litov, B. Pavlov, P. Petkov, A. Petrov

Beihang University, Beijing, China

W. Fang³, Q. Guo, H. Wang, L. Yuan

Department of Physics, Tsinghua University, Beijing, China

M. Ahmad, Z. Hu, Y. Wang, K. Yi⁹

Institute of High Energy Physics, Beijing, China

E. Chapon, G.M. Chen¹⁰, H.S. Chen¹⁰, M. Chen, T. Javaid¹⁰, A. Kapoor, D. Leggat, H. Liao, Z. Liu, R. Sharma, A. Spiezia, J. Tao, J. Thomas-Wilsker, J. Wang, H. Zhang, S. Zhang¹⁰, J. Zhao

State Key Laboratory of Nuclear Physics and Technology, Peking University, Beijing, China

A. Agapitos, Y. Ban, C. Chen, Q. Huang, A. Levin, Q. Li, M. Lu, X. Lyu, Y. Mao, S.J. Qian, D. Wang, Q. Wang, J. Xiao

Sun Yat-Sen University, Guangzhou, China

Z. You

Institute of Modern Physics and Key Laboratory of Nuclear Physics and Ion-beam Application (MOE) - Fudan University, Shanghai, China

X. Gao³

Zhejiang University, Hangzhou, China

M. Xiao

Universidad de Los Andes, Bogota, Colombia

C. Avila, A. Cabrera, C. Florez, J. Fraga, A. Sarkar, M.A. Segura Delgado

Universidad de Antioquia, Medellin, Colombia

J. Jaramillo, J. Mejia Guisao, F. Ramirez, J.D. Ruiz Alvarez, C.A. Salazar González, N. Vanegas Arbelaez

University of Split, Faculty of Electrical Engineering, Mechanical Engineering and Naval Architecture, Split, Croatia

D. Giljanovic, N. Godinovic, D. Lelas, I. Puljak

University of Split, Faculty of Science, Split, Croatia

Z. Antunovic, M. Kovac, T. Sculac

Institute Rudjer Boskovic, Zagreb, Croatia

V. Brigljevic, D. Ferencek, D. Majumder, M. Roguljic, A. Starodumov¹¹, T. Susa

University of Cyprus, Nicosia, Cyprus

M.W. Ather, A. Attikis, E. Erodotou, A. Ioannou, G. Kole, M. Kolosova, S. Konstantinou, J. Mousa, C. Nicolaou, F. Ptochos, P.A. Razis, H. Rykaczewski, H. Saka, D. Tsiakkouri

Charles University, Prague, Czech Republic
M. Finger¹², M. Finger Jr.¹², A. Kveton, J. Tomsa

Escuela Politecnica Nacional, Quito, Ecuador
E. Ayala

Universidad San Francisco de Quito, Quito, Ecuador
E. Carrera Jarrin

**Academy of Scientific Research and Technology of the Arab Republic of Egypt,
Egyptian Network of High Energy Physics, Cairo, Egypt**
A.A. Abdelalim^{13,14}, Y. Assran^{15,16}, E. Salama^{16,17}

**Center for High Energy Physics (CHEP-FU), Fayoum University, El-Fayoum,
Egypt**

M.A. Mahmoud, Y. Mohammed

National Institute of Chemical Physics and Biophysics, Tallinn, Estonia
S. Bhowmik, A. Carvalho Antunes De Oliveira, R.K. Dewanjee, K. Ehataht, M. Kadastik,
M. Raidal, C. Veelken

Department of Physics, University of Helsinki, Helsinki, Finland
P. Eerola, L. Forthomme, H. Kirschenmann, K. Osterberg, M. Voutilainen

Helsinki Institute of Physics, Helsinki, Finland

E. Brückner, F. Garcia, J. Havukainen, V. Karimäki, M.S. Kim, R. Kinnunen, T. Lampén,
K. Lassila-Perini, S. Lehti, T. Lindén, H. Siikonen, E. Tuominen, J. Tuominiemi

Lappeenranta University of Technology, Lappeenranta, Finland
P. Luukka, T. Tuuva

IRFU, CEA, Université Paris-Saclay, Gif-sur-Yvette, France
C. Amendola, M. Besancon, F. Couderc, M. Dejardin, D. Denegri, J.L. Faure, F. Ferri,
S. Ganjour, A. Givernaud, P. Gras, G. Hamel de Monchenault, P. Jarry, B. Lenzi, E. Locci,
J. Malcles, J. Rander, A. Rosowsky, M.Ö. Sahin, A. Savoy-Navarro¹⁸, M. Titov, G.B. Yu

**Laboratoire Leprince-Ringuet, CNRS/IN2P3, Ecole Polytechnique, Institut
Polytechnique de Paris, Palaiseau, France**

S. Ahuja, F. Beaudette, M. Bonanomi, A. Buchot Perragin, P. Busson, C. Charlot,
O. Davignon, B. Diab, G. Falmagne, R. Granier de Cassagnac, A. Hakimi, I. Kucher,
A. Lobanova, C. Martin Perez, M. Nguyen, C. Ochando, P. Paganini, J. Rembser, R. Salerno,
J.B. Sauvan, Y. Sirois, A. Zabi, A. Zghiche

Université de Strasbourg, CNRS, IPHC UMR 7178, Strasbourg, France
J.-L. Agram¹⁹, J. Andrea, D. Bloch, G. Bourgat, J.-M. Brom, E.C. Chabert, C. Collard,
J.-C. Fontaine¹⁹, D. Gelé, U. Goerlach, C. Grimault, A.-C. Le Bihan, P. Van Hove

**Université de Lyon, Université Claude Bernard Lyon 1, CNRS-IN2P3, Institut
de Physique Nucléaire de Lyon, Villeurbanne, France**

E. Asilar, S. Beauceron, C. Bernet, G. Boudoul, C. Camen, A. Carle, N. Chanon, D. Contardo,
P. Depasse, H. El Mamouni, J. Fay, S. Gascon, M. Gouzevitch, B. Ille, Sa. Jain,
I.B. Laktineh, H. Lattaud, A. Lesauvage, M. Lethuillier, L. Mirabito, L. Torterotot,
G. Touquet, M. Vander Donckt, S. Viret

Georgian Technical University, Tbilisi, GeorgiaA. Khvedelidze¹², Z. Tsamalaidze¹²**RWTH Aachen University, I. Physikalisches Institut, Aachen, Germany**

L. Feld, K. Klein, M. Lipinski, D. Meuser, A. Pauls, M. Preuten, M.P. Rauch, J. Schulz, M. Teroerde

RWTH Aachen University, III. Physikalisches Institut A, Aachen, Germany

D. Eliseev, M. Erdmann, P. Fackeldey, B. Fischer, S. Ghosh, T. Hebbeker, K. Hoepfner, H. Keller, L. Mastrolorenzo, M. Merschmeyer, A. Meyer, G. Mocellin, S. Mondal, S. Mukherjee, D. Noll, A. Novak, T. Pook, A. Pozdnyakov, Y. Rath, H. Reithler, J. Roemer, A. Schmidt, S.C. Schuler, A. Sharma, S. Wiedenbeck, S. Zaleski

RWTH Aachen University, III. Physikalisches Institut B, Aachen, GermanyC. Dziwok, G. Flügge, W. Haj Ahmad²⁰, O. Hlushchenko, T. Kress, A. Nowack, C. Pistone, O. Pooth, D. Roy, H. Sert, A. Stahl²¹, T. Ziemons**Deutsches Elektronen-Synchrotron, Hamburg, Germany**H. Aarup Petersen, M. Aldaya Martin, P. Asmuss, I. Babounikau, S. Baxter, O. Behnke, A. Bermúdez Martínez, A.A. Bin Anuar, K. Borras²², V. Botta, D. Brunner, A. Campbell, A. Cardini, P. Connor, S. Consuegra Rodríguez, V. Danilov, A. De Wit, M.M. Deffranchis, L. Didukh, D. Domínguez Damiani, G. Eckerlin, D. Eckstein, T. Eichhorn, L.I. Estevez Banos, E. Gallo²³, A. Geiser, A. Giraldi, A. Grohsjean, M. Guthoff, A. Harb, A. Jafari²⁴, N.Z. Jomhari, H. Jung, A. Kasem²², M. Kasemann, H. Kaveh, C. Kleinwort, J. Knolle, D. Krücker, W. Lange, T. Lenz, J. Lidrych, K. Lipka, W. Lohmann²⁵, R. Mankel, I.-A. Melzer-Pellmann, J. Metwally, A.B. Meyer, M. Meyer, M. Missiroli, J. Mnich, A. Mussgiller, V. Myronenko, Y. Otarid, D. Pérez Adán, S.K. Pflitsch, D. Pitzl, A. Raspareza, A. Saggio, A. Saibel, M. Savitskyi, V. Scheurer, C. Schwanenberger, A. Singh, R.E. Sosa Ricardo, N. Tonon, O. Turkot, A. Vagnerini, M. Van De Klundert, R. Walsh, D. Walter, Y. Wen, K. Wichmann, C. Wissing, S. Wuchterl, O. Zenaiev, R. Zlebcik**University of Hamburg, Hamburg, Germany**

R. Aggleton, S. Bein, L. Benato, A. Benecke, K. De Leo, T. Dreyer, A. Ebrahimi, M. Eich, F. Feindt, A. Fröhlich, C. Garbers, E. Garutti, P. Gunnellini, J. Haller, A. Hinzmamn, A. Karavdina, G. Kasieczka, R. Klanner, R. Kogler, V. Kutzner, J. Lange, T. Lange, A. Malara, C.E.N. Niemeyer, A. Nigamova, K.J. Pena Rodriguez, O. Rieger, P. Schleper, S. Schumann, J. Schwandt, D. Schwarz, J. Sonneveld, H. Stadie, G. Steinbrück, B. Vormwald, I. Zoi

Karlsruher Institut fuer Technologie, Karlsruhe, GermanyJ. Bechtel, T. Berger, E. Butz, R. Caspart, T. Chwalek, W. De Boer, A. Dierlamm, A. Droll, K. El Morabit, N. Faltermann, K. Flöh, M. Giffels, A. Gottmann, F. Hartmann²¹, C. Heidecker, U. Husemann, M.A. Iqbal, I. Katkov²⁶, P. Keicher, R. Koppenhöfer, S. Maier, M. Metzler, S. Mitra, D. Müller, Th. Müller, M. Musich, G. Quast, K. Rabbertz, J. Rauser, D. Savoiu, D. Schäfer, M. Schnepf, M. Schröder, D. Seith, I. Shvetsov, H.J. Simonis, R. Ulrich, M. Wassmer, M. Weber, R. Wolf, S. Wozniewski

Institute of Nuclear and Particle Physics (INPP), NCSR Demokritos, Aghia Paraskevi, Greece

G. Anagnostou, P. Asenov, G. Daskalakis, T. Geralis, A. Kyriakis, D. Loukas, G. Paspalaki, A. Stakia

National and Kapodistrian University of Athens, Athens, Greece

M. Diamantopoulou, D. Karasavvas, G. Karathanasis, P. Kontaxakis, C.K. Koraka, A. Manousakis-Katsikakis, A. Panagiotou, I. Papavergou, N. Saoulidou, K. Theofilatos, K. Vellidis, E. Vourliotis

National Technical University of Athens, Athens, Greece

G. Bakas, K. Kousouris, I. Papakrivopoulos, G. Tsipolitis, A. Zacharopoulos

University of Ioánnina, Ioánnina, Greece

I. Evangelou, C. Foudas, P. Gianneios, P. Katsoulis, P. Kokkas, K. Manitara, N. Manthos, I. Papadopoulos, J. Strologas

MTA-ELTE Lendület CMS Particle and Nuclear Physics Group, Eötvös Loránd University, Budapest, Hungary

M. Bartók²⁷, M. Csanad, M.M.A. Gadallah²⁸, S. Lökö²⁹, P. Major, K. Mandal, A. Mehta, G. Pasztor, O. Surányi, G.I. Veres

Wigner Research Centre for Physics, Budapest, Hungary

G. Bencze, C. Hajdu, D. Horvath³⁰, F. Sikler, V. Veszpremi, G. Vesztergombi[†]

Institute of Nuclear Research ATOMKI, Debrecen, Hungary

S. Czellar, J. Karancsi²⁷, J. Molnar, Z. Szillasi, D. Teyssier

Institute of Physics, University of Debrecen, Debrecen, Hungary

P. Raics, Z.L. Trocsanyi, B. Ujvari

Eszterhazy Karoly University, Karoly Robert Campus, Gyongyos, Hungary

T. Csorgo, F. Nemes, T. Novak

Indian Institute of Science (IISc), Bangalore, India

S. Choudhury, J.R. Komaragiri, D. Kumar, L. Panwar, P.C. Tiwari

National Institute of Science Education and Research, HBNI, Bhubaneswar, India

S. Bahinipati³¹, D. Dash, C. Kar, P. Mal, T. Mishra, V.K. Muraleedharan Nair Bindhu, A. Nayak³², D.K. Sahoo³¹, N. Sur, S.K. Swain

Punjab University, Chandigarh, India

S. Bansal, S.B. Beri, V. Bhatnagar, G. Chaudhary, S. Chauhan, N. Dhingra³³, R. Gupta, A. Kaur, S. Kaur, P. Kumari, M. Meena, K. Sandeep, S. Sharma, J.B. Singh, A.K. Virdi

University of Delhi, Delhi, India

A. Ahmed, A. Bhardwaj, B.C. Choudhary, R.B. Garg, M. Gola, S. Keshri, A. Kumar, M. Naimuddin, P. Priyanka, K. Ranjan, A. Shah

Saha Institute of Nuclear Physics, HBNI, Kolkata, India

M. Bharti³⁴, R. Bhattacharya, S. Bhattacharya, D. Bhowmik, S. Dutta, S. Ghosh, B. Gomber³⁵, M. Maity³⁶, S. Nandan, P. Palit, P.K. Rout, G. Saha, B. Sahu, S. Sarkar, M. Sharan, B. Singh³⁴, S. Thakur³⁴

Indian Institute of Technology Madras, Madras, India

P.K. Behera, S.C. Behera, P. Kalbhor, A. Muhammad, R. Pradhan, P.R. Pujahari, A. Sharma, A.K. Sikdar

Bhabha Atomic Research Centre, Mumbai, India

D. Dutta, V. Kumar, K. Naskar³⁷, P.K. Netrakanti, L.M. Pant, P. Shukla

Tata Institute of Fundamental Research-A, Mumbai, India

T. Aziz, M.A. Bhat, S. Dugad, R. Kumar Verma, G.B. Mohanty, U. Sarkar

Tata Institute of Fundamental Research-B, Mumbai, India

S. Banerjee, S. Bhattacharya, S. Chatterjee, R. Chudasama, M. Guchait, S. Karmakar, S. Kumar, G. Majumder, K. Mazumdar, S. Mukherjee, D. Roy

Indian Institute of Science Education and Research (IISER), Pune, India

S. Dube, B. Kansal, S. Pandey, A. Rane, A. Rastogi, S. Sharma

Department of Physics, Isfahan University of Technology, Isfahan, Iran

H. Bakhshiansohi³⁸, M. Zeinali³⁹

Institute for Research in Fundamental Sciences (IPM), Tehran, Iran

S. Chenarani⁴⁰, S.M. Etesami, M. Khakzad, M. Mohammadi Najafabadi

University College Dublin, Dublin, Ireland

M. Felcini, M. Grunewald

INFN Sezione di Bari ^a, Università di Bari ^b, Politecnico di Bari ^c, Bari, Italy

M. Abbrescia^{a,b}, R. Aly^{a,b,41}, C. Aruta^{a,b}, A. Colaleo^a, D. Creanza^{a,c}, N. De Filippis^{a,c}, M. De Palma^{a,b}, A. Di Florio^{a,b}, A. Di Pilato^{a,b}, W. Elmetenawee^{a,b}, L. Fiore^a, A. Gelmi^{a,b}, M. Gul^a, G. Iaselli^{a,c}, M. Ince^{a,b}, S. Lezki^{a,b}, G. Maggi^{a,c}, M. Maggi^a, I. Margjeka^{a,b}, V. Mastrapasqua^{a,b}, J.A. Merlin^a, S. My^{a,b}, S. Nuzzo^{a,b}, A. Pompili^{a,b}, G. Pugliese^{a,c}, A. Ranieri^a, G. Selvaggi^{a,b}, L. Silvestris^a, F.M. Simone^{a,b}, R. Venditti^a, P. Verwilligen^a

INFN Sezione di Bologna ^a, Università di Bologna ^b, Bologna, Italy

G. Abbiendi^a, C. Battilana^{a,b}, D. Bonacorsi^{a,b}, L. Borgonovi^a, S. Braibant-Giacomelli^{a,b}, R. Campanini^{a,b}, P. Capiluppi^{a,b}, A. Castro^{a,b}, F.R. Cavallo^a, C. Ciocca^a, M. Cuffiani^{a,b}, G.M. Dallavalle^a, T. Diotalevi^{a,b}, F. Fabbri^a, A. Fanfani^{a,b}, E. Fontanesi^{a,b}, P. Giacomelli^a, L. Giommi^{a,b}, C. Grandi^a, L. Guiducci^{a,b}, F. Iemmi^{a,b}, S. Lo Meo^{a,42}, S. Marcellini^a, G. Masetti^a, F.L. Navarria^{a,b}, A. Perrotta^a, F. Primavera^{a,b}, A.M. Rossi^{a,b}, T. Rovelli^{a,b}, G.P. Siroli^{a,b}, N. Tosi^a

INFN Sezione di Catania ^a, Università di Catania ^b, Catania, Italy

S. Albergo^{a,b,43}, S. Costa^{a,b,43}, A. Di Mattia^a, R. Potenza^{a,b}, A. Tricomi^{a,b,43}, C. Tuve^{a,b}

INFN Sezione di Firenze ^a, Università di Firenze ^b, Firenze, Italy

G. Barbagli^a, A. Cassese^a, R. Ceccarelli^{a,b}, V. Ciulli^{a,b}, C. Civinini^a, R. D'Alessandro^{a,b}, F. Fiori^a, E. Focardi^{a,b}, G. Latino^{a,b}, P. Lenzi^{a,b}, M. Lizzo^{a,b}, M. Meschini^a, S. Paoletti^a, R. Seidita^{a,b}, G. Sguazzoni^a, L. Viliani^a

INFN Laboratori Nazionali di Frascati, Frascati, Italy

L. Benussi, S. Bianco, D. Piccolo

INFN Sezione di Genova ^a, Università di Genova ^b, Genova, Italy

M. Bozzo^{a,b}, F. Ferro^a, R. Mulargia^{a,b}, E. Robutti^a, S. Tosi^{a,b}

INFN Sezione di Milano-Bicocca ^a, Università di Milano-Bicocca ^b, Milano, Italy

A. Benaglia^a, A. Beschi^{a,b}, F. Brivio^{a,b}, F. Cetorelli^{a,b}, V. Ciriolo^{a,b,21}, F. De Guio^{a,b}, M.E. Dinardo^{a,b}, P. Dini^a, S. Gennai^a, A. Ghezzi^{a,b}, P. Govoni^{a,b}, L. Guzzi^{a,b}, M. Malberti^a, S. Malvezzi^a, A. Massironi^a, D. Menasce^a, F. Monti^{a,b}, L. Moroni^a, M. Paganoni^{a,b}, D. Pedrini^a, S. Ragazzi^{a,b}, T. Tabarelli de Fatis^{a,b}, D. Valsecchi^{a,b,21}, D. Zuolo^{a,b}

INFN Sezione di Napoli ^a, Università di Napoli 'Federico II' ^b, Napoli, Italy, Università della Basilicata ^c, Potenza, Italy, Università G. Marconi ^d, Roma, Italy

S. Buontempo^a, N. Cavallo^{a,c}, A. De Iorio^{a,b}, F. Fabozzi^{a,c}, F. Fienga^a, A.O.M. Iorio^{a,b}, L. Lista^{a,b}, S. Meola^{a,d,21}, P. Paolucci^{a,21}, B. Rossi^a, C. Sciacca^{a,b}, E. Voevodina^{a,b}

INFN Sezione di Padova ^a, Università di Padova ^b, Padova, Italy, Università di Trento ^c, Trento, Italy

P. Azzi^a, N. Bacchetta^a, D. Bisello^{a,b}, P. Bortignon^a, A. Bragagnolo^{a,b}, R. Carlin^{a,b}, P. Checchia^a, P. De Castro Manzano^a, T. Dorigo^a, F. Gasparini^{a,b}, U. Gasparini^{a,b}, S.Y. Hoh^{a,b}, L. Layer^{a,44}, M. Margoni^{a,b}, A.T. Meneguzzo^{a,b}, M. Presilla^{a,b}, P. Ronchese^{a,b}, R. Rossin^{a,b}, F. Simonetto^{a,b}, G. Strong^a, M. Tosi^{a,b}, H. Yarar^{a,b}, M. Zanetti^{a,b}, P. Zotto^{a,b}, A. Zucchetta^{a,b}, G. Zumerle^{a,b}

INFN Sezione di Pavia ^a, Università di Pavia ^b, Pavia, Italy

C. Aime^{a,b}, A. Braghieri^a, S. Calzaferri^{a,b}, D. Fiorina^{a,b}, P. Montagna^{a,b}, S.P. Ratti^{a,b}, V. Re^a, M. Ressegotti^{a,b}, C. Riccardi^{a,b}, P. Salvini^a, I. Vai^a, P. Vitulo

INFN Sezione di Perugia ^a, Università di Perugia ^b, Perugia, Italy

M. Biasini^{a,b}, G.M. Bilei^a, D. Ciangottini^{a,b}, L. Fanò^{a,b}, P. Lariccia^{a,b}, G. Mantovani^{a,b}, V. Mariani^{a,b}, M. Menichelli^a, F. Moscatelli^a, A. Piccinelli^{a,b}, A. Rossi^{a,b}, A. Santocchia^{a,b}, D. Spiga^a, T. Tedeschi^{a,b}

INFN Sezione di Pisa ^a, Università di Pisa ^b, Scuola Normale Superiore di Pisa ^c, Pisa Italy, Università di Siena ^d, Siena, Italy

K. Androsov^a, P. Azzurri^a, G. Bagliesi^a, V. Bertacchi^{a,c}, L. Bianchini^a, T. Boccali^a, R. Castaldi^a, M.A. Ciocci^{a,b}, R. Dell'Orso^a, M.R. Di Domenico^{a,d}, S. Donato^a, L. Giannini^{a,c}, A. Giassi^a, M.T. Grippo^a, F. Ligabue^{a,c}, E. Manca^{a,c}, G. Mandorli^{a,c}, A. Messineo^{a,b}, F. Palla^a, G. Ramirez-Sanchez^{a,c}, A. Rizzi^{a,b}, G. Rolandi^{a,c}, S. Roy Chowdhury^{a,c}, A. Scribano^a, N. Shafiei^{a,b}, P. Spagnolo^a, R. Tenchini^a, G. Tonelli^{a,b}, N. Turini^{a,d}, A. Venturi^a, P.G. Verdini^a

INFN Sezione di Roma ^a, Sapienza Università di Roma ^b, Rome, Italy

F. Cavallari^a, M. Cipriani^{a,b}, D. Del Re^{a,b}, E. Di Marco^a, M. Diemoz^a, E. Longo^{a,b}, P. Meridiani^a, G. Organtini^{a,b}, F. Pandolfi^a, R. Paramatti^{a,b}, C. Quaranta^{a,b}, S. Rahatlou^{a,b}, C. Rovelli^a, F. Santanastasio^{a,b}, L. Soffi^{a,b}, R. Tramontano^{a,b}

INFN Sezione di Torino ^a, Università di Torino ^b, Torino, Italy, Università del Piemonte Orientale ^c, Novara, Italy

N. Amapane^{a,b}, R. Arcidiacono^{a,c}, S. Argiro^{a,b}, M. Arneodo^{a,c}, N. Bartosik^a, R. Bellan^{a,b}, A. Bellora^{a,b}, J. Berenguer Antequera^{a,b}, C. Biino^a, A. Cappati^{a,b}, N. Cartiglia^a, S. Cometti^a, M. Costa^{a,b}, R. Covarelli^{a,b}, N. Demaria^a, B. Kiani^{a,b}, F. Legger^a, C. Mariotti^a, S. Maselli^a, E. Migliore^{a,b}, V. Monaco^{a,b}, E. Monteil^{a,b},

M. Monteno^a, M.M. Obertino^{a,b}, G. Ortona^a, L. Pacher^{a,b}, N. Pastrone^a, M. Pelliccioni^a, G.L. Pinna Angioni^{a,b}, M. Ruspa^{a,c}, R. Salvatico^{a,b}, F. Siviero^{a,b}, V. Sola^a, A. Solano^{a,b}, D. Soldi^{a,b}, A. Staiano^a, M. Tornago^{a,b}, D. Trocino^{a,b}

INFN Sezione di Trieste ^a, Università di Trieste ^b, Trieste, Italy

S. Belforte^a, V. Candelise^{a,b}, M. Casarsa^a, F. Cossutti^a, A. Da Rold^{a,b}, G. Della Ricca^{a,b}, F. Vazzoler^{a,b}

Kyungpook National University, Daegu, Korea

S. Dogra, C. Huh, B. Kim, D.H. Kim, G.N. Kim, J. Lee, S.W. Lee, C.S. Moon, Y.D. Oh, S.I. Pak, B.C. Radburn-Smith, S. Sekmen, Y.C. Yang

Chonnam National University, Institute for Universe and Elementary Particles, Kwangju, Korea

H. Kim, D.H. Moon

Hanyang University, Seoul, Korea

B. Francois, T.J. Kim, J. Park

Korea University, Seoul, Korea

S. Cho, S. Choi, Y. Go, S. Ha, B. Hong, K. Lee, K.S. Lee, J. Lim, J. Park, S.K. Park, J. Yoo

Kyung Hee University, Department of Physics, Seoul, Republic of Korea

J. Goh, A. Gurtu

Sejong University, Seoul, Korea

H.S. Kim, Y. Kim

Seoul National University, Seoul, Korea

J. Almond, J.H. Bhyun, J. Choi, S. Jeon, J. Kim, J.S. Kim, S. Ko, H. Kwon, H. Lee, K. Lee, S. Lee, K. Nam, B.H. Oh, M. Oh, S.B. Oh, H. Seo, U.K. Yang, I. Yoon

University of Seoul, Seoul, Korea

D. Jeon, J.H. Kim, B. Ko, J.S.H. Lee, I.C. Park, Y. Roh, D. Song, I.J. Watson

Yonsei University, Department of Physics, Seoul, Korea

H.D. Yoo

Sungkyunkwan University, Suwon, Korea

Y. Choi, C. Hwang, Y. Jeong, H. Lee, Y. Lee, I. Yu

College of Engineering and Technology, American University of the Middle East (AUM), Dasman, Kuwait

Y. Maghrbi

Riga Technical University, Riga, Latvia

V. Veckalns⁴⁵

Vilnius University, Vilnius, Lithuania

A. Juodagalvis, A. Rinkevicius, G. Tamulaitis, A. Vaitkevicius

National Centre for Particle Physics, Universiti Malaya, Kuala Lumpur, Malaysia

W.A.T. Wan Abdullah, M.N. Yusli, Z. Zolkapli

Universidad de Sonora (UNISON), Hermosillo, Mexico

J.F. Benitez, A. Castaneda Hernandez, J.A. Murillo Quijada, L. Valencia Palomo

Centro de Investigacion y de Estudios Avanzados del IPN, Mexico City, MexicoG. Ayala, H. Castilla-Valdez, E. De La Cruz-Burelo, I. Heredia-De La Cruz⁴⁶, R. Lopez-Fernandez, C.A. Mondragon Herrera, D.A. Perez Navarro, A. Sanchez-Hernandez**Universidad Iberoamericana, Mexico City, Mexico**

S. Carrillo Moreno, C. Oropeza Barrera, M. Ramirez-Garcia, F. Vazquez Valencia

Benemerita Universidad Autonoma de Puebla, Puebla, Mexico

J. Eysermans, I. Pedraza, H.A. Salazar Ibarguen, C. Uribe Estrada

Universidad Autónoma de San Luis Potosí, San Luis Potosí, Mexico

A. Morelos Pineda

University of Montenegro, Podgorica, MontenegroJ. Mijuskovic⁴, N. Raicevic**University of Auckland, Auckland, New Zealand**

D. Krovcheck

University of Canterbury, Christchurch, New Zealand

S. Bheesette, P.H. Butler

National Centre for Physics, Quaid-I-Azam University, Islamabad, Pakistan

A. Ahmad, M.I. Asghar, A. Awais, M.I.M. Awan, H.R. Hoorani, W.A. Khan, M.A. Shah, M. Shoaib, M. Waqas

AGH University of Science and Technology Faculty of Computer Science, Electronics and Telecommunications, Krakow, Poland

V. Avati, L. Grzanka, M. Malawski

National Centre for Nuclear Research, Swierk, Poland

H. Bialkowska, M. Bluj, B. Boimska, T. Frueboes, M. Górski, M. Kazana, M. Szleper, P. Traczyk, P. Zalewski

Institute of Experimental Physics, Faculty of Physics, University of Warsaw, Warsaw, Poland

K. Bunkowski, K. Doroba, A. Kalinowski, M. Konecki, J. Krolikowski, M. Walczak

Laboratório de Instrumentação e Física Experimental de Partículas, Lisboa, Portugal

M. Araujo, P. Bargassa, D. Bastos, A. Boletti, P. Faccioli, M. Gallinaro, J. Hollar, N. Leonardo, T. Niknejad, J. Seixas, K. Shchelina, O. Toldaiev, J. Varela

Joint Institute for Nuclear Research, Dubna, RussiaS. Afanasiev, P. Bunin, M. Gavrilenko, I. Golutvin, I. Gorbunov, A. Kamenev, V. Karjavine, A. Lanev, A. Malakhov, V. Matveev^{47,48}, V. Palichik, V. Perelygin, M. Savina, V. Shalaev, S. Shmatov, S. Shulha, V. Smirnov, O. Teryaev, N. Voytishin, B.S. Yuldashev⁴⁹, A. Zarubin, I. Zhizhin**Petersburg Nuclear Physics Institute, Gatchina (St. Petersburg), Russia**G. Gavrilov, V. Golovtcov, Y. Ivanov, V. Kim⁵⁰, E. Kuznetsova⁵¹, V. Murzin, V. Oreshkin, I. Smirnov, D. Sosnov, V. Sulimov, L. Uvarov, S. Volkov, A. Vorobyev

Institute for Nuclear Research, Moscow, Russia

Yu. Andreev, A. Dermenev, S. Glinenko, N. Golubev, A. Karneyeu, M. Kirsanov,
N. Krasnikov, A. Pashenkov, G. Pivovarov, D. Tlisov[†], A. Toropin

**Institute for Theoretical and Experimental Physics named by A.I. Alikhanov
of NRC ‘Kurchatov Institute’, Moscow, Russia**

V. Epshteyn, V. Gavrilov, N. Lychkovskaya, A. Nikitenko⁵², V. Popov, G. Safronov,
A. Spiridonov, A. Stepennov, M. Toms, E. Vlasov, A. Zhokin

Moscow Institute of Physics and Technology, Moscow, Russia

T. Aushev

**National Research Nuclear University ‘Moscow Engineering Physics Institute’
(MEPhI), Moscow, Russia**

O. Bychkova, M. Chadeeva⁵³, D. Philippov, E. Popova, V. Rusinov

P.N. Lebedev Physical Institute, Moscow, Russia

V. Andreev, M. Azarkin, I. Dremin, M. Kirakosyan, A. Terkulov

**Skobeltsyn Institute of Nuclear Physics, Lomonosov Moscow State University,
Moscow, Russia**

A. Belyaev, E. Boos, A. Ershov, A. Gribushin, A. Kaminskiy⁵⁴, O. Kodolova, V. Korotkikh,
I. Loktin, S. Obraztsov, S. Petrushanko, V. Savrin, A. Snigirev, I. Vardanyan

Novosibirsk State University (NSU), Novosibirsk, Russia

V. Blinov⁵⁵, T. Dimova⁵⁵, L. Kardapoltsev⁵⁵, I. Ovtin⁵⁵, Y. Skovpen⁵⁵

**Institute for High Energy Physics of National Research Centre ‘Kurchatov
Institute’, Protvino, Russia**

I. Azhgirey, I. Bayshev, V. Kachanov, A. Kalinin, D. Konstantinov, V. Petrov, R. Ryutin,
A. Sobol, S. Troshin, N. Tyurin, A. Uzunian, A. Volkov

National Research Tomsk Polytechnic University, Tomsk, Russia

A. Babaev, A. Iuzhakov, V. Okhotnikov, L. Sukhikh

Tomsk State University, Tomsk, Russia

V. Borchsh, V. Ivanchenko, E. Tcherniaev

**University of Belgrade: Faculty of Physics and VINCA Institute of Nuclear
Sciences, Belgrade, Serbia**

P. Adzic⁵⁶, P. Cirkovic, M. Dordevic, P. Milenovic, J. Milosevic

**Centro de Investigaciones Energéticas Medioambientales y Tecnológicas
(CIEMAT), Madrid, Spain**

M. Aguilar-Benitez, J. Alcaraz Maestre, A. Álvarez Fernández, I. Bachiller, M. Barrio Luna, Cristina F. Bedoya, J.A. Brochero Cifuentes, C.A. Carrillo Montoya, M. Cepeda, M. Cerrada, N. Colino, B. De La Cruz, A. Delgado Peris, J.P. Fernández Ramos, J. Flix, M.C. Fouz, A. García Alonso, O. Gonzalez Lopez, S. Goy Lopez, J.M. Hernandez, M.I. Josa, J. León Holgado, D. Moran, Á. Navarro Tobar, A. Pérez-Calero Yzquierdo, J. Puerta Pelayo, I. Redondo, L. Romero, S. Sánchez Navas, M.S. Soares, A. Triossi, L. Urda Gómez, C. Willmott

Universidad Autónoma de Madrid, Madrid, Spain

C. Albajar, J.F. de Trocóniz, R. Reyes-Almanza

Universidad de Oviedo, Instituto Universitario de Ciencias y Tecnologías Espaciales de Asturias (ICTEA), Oviedo, Spain

B. Alvarez Gonzalez, J. Cuevas, C. Erice, J. Fernandez Menendez, S. Folgueras, I. Gonzalez Caballero, E. Palencia Cortezon, C. Ramón Álvarez, J. Ripoll Sau, V. Rodríguez Bouza, S. Sanchez Cruz, A. Trapote

Instituto de Física de Cantabria (IFCA), CSIC-Universidad de Cantabria, Santander, Spain

I.J. Cabrillo, A. Calderon, B. Chazin Quero, J. Duarte Campderros, M. Fernandez, P.J. Fernández Manteca, G. Gomez, C. Martinez Rivero, P. Martinez Ruiz del Arbol, F. Matorras, J. Piedra Gomez, C. Prieels, F. Ricci-Tam, T. Rodrigo, A. Ruiz-Jimeno, L. Scodellaro, I. Vila, J.M. Vizan Garcia

University of Colombo, Colombo, Sri Lanka

M.K. Jayananda, B. Kailasapathy⁵⁷, D.U.J. Sonnadara, D.D.C. Wickramarathna

University of Ruhuna, Department of Physics, Matara, Sri Lanka

W.G.D. Dharmaratna, K. Liyanage, N. Perera, N. Wickramage

CERN, European Organization for Nuclear Research, Geneva, Switzerland

T.K. Arrestad, D. Abbaneo, B. Akgun, E. Auffray, G. Auzinger, J. Baechler, P. Baillon, A.H. Ball, D. Barney, J. Bendavid, N. Beni, M. Bianco, A. Bocci, E. Bossini, E. Brondolin, T. Camporesi, M. Capeans Garrido, G. Cerminara, L. Cristella, D. d'Enterria, A. Dabrowski, N. Daci, V. Daponte, A. David, A. De Roeck, M. Deile, R. Di Maria, M. Dobson, M. Dünser, N. Dupont, A. Elliott-Peisert, N. Emriskova, F. Fallavollita⁵⁸, D. Fasanella, S. Fiorendi, A. Florent, G. Franzoni, J. Fulcher, W. Funk, S. Giani, D. Gigi, K. Gill, F. Glege, L. Gouskos, M. Guilbaud, D. Gulhan, M. Haranko, J. Hege-man, Y. Iiyama, V. Innocente, T. James, P. Janot, J. Kaspar, J. Kieseler, M. Komm, N. Kratochwil, C. Lange, S. Laurila, P. Lecoq, K. Long, C. Lourenço, L. Malgeri, S. Mallios, M. Mannelli, F. Meijers, S. Mersi, E. Meschi, F. Moortgat, M. Mulders, J. Niedziela, S. Orfanelli, L. Orsini, F. Pantaleo²¹, L. Pape, E. Perez, M. Peruzzi, A. Petrilli, G. Petrucciani, A. Pfeiffer, M. Pierini, T. Quast, D. Rabady, A. Racz, M. Rieger, M. Rovere, H. Sakulin, J. Salfeld-Nebgen, S. Scarfi, C. Schäfer, C. Schwick, M. Selvaggi, A. Sharma, P. Silva, W. Snoeys, P. Sphicas⁵⁹, S. Summers, V.R. Tavolaro, D. Treille, A. Tsirou, G.P. Van Onsem, A. Vartak, M. Verzetti, K.A. Wozniak, W.D. Zeuner

Paul Scherrer Institut, Villigen, Switzerland

L. Caminada⁶⁰, W. Erdmann, R. Horisberger, Q. Ingram, H.C. Kaestli, D. Kotlinski, U. Langenegger, T. Rohe

ETH Zurich - Institute for Particle Physics and Astrophysics (IPA), Zurich, Switzerland

M. Backhaus, P. Berger, A. Calandri, N. Chernyavskaya, A. De Cosa, G. Dissertori, M. Dittmar, M. Donegà, C. Dorfer, T. Gadek, T.A. Gómez Espinosa, C. Grab, D. Hits, W. Lustermann, A.-M. Lyon, R.A. Manzoni, M.T. Meinhard, F. Micheli, F. Nessi-Tedaldi, F. Pauss, V. Perovic, G. Perrin, S. Pigazzini, M.G. Ratti, M. Reichmann, C. Reissel, T. Reitenspiess, B. Ristic, D. Ruini, D.A. Sanz Becerra, M. Schönenberger, V. Stampf, J. Steggemann⁶¹, M.L. Vesterbacka Olsson, R. Wallny, D.H. Zhu

Universität Zürich, Zurich, Switzerland

C. Amsler⁶², C. Botta, D. Brzhechko, M.F. Canelli, R. Del Burgo, J.K. Heikkilä, M. Huwiler, A. Jofrehei, B. Kilminster, S. Leontsinis, A. Macchiolo, P. Meiring, V.M. Mikuni, U. Molinatti, I. Neutelings, G. Rauco, A. Reimers, P. Robmann, K. Schweiger, Y. Takahashi

National Central University, Chung-Li, Taiwan

C. Adloff⁶³, C.M. Kuo, W. Lin, A. Roy, T. Sarkar³⁶, S.S. Yu

National Taiwan University (NTU), Taipei, Taiwan

L. Ceard, P. Chang, Y. Chao, K.F. Chen, P.H. Chen, W.-S. Hou, Y.y. Li, R.-S. Lu, E. Paganis, A. Psallidas, A. Steen, E. Yazgan

Chulalongkorn University, Faculty of Science, Department of Physics, Bangkok, Thailand

B. Asavapibhop, C. Asawatangtrakuldee, N. Srimanobhas

Çukurova University, Physics Department, Science and Art Faculty, Adana, Turkey

F. Boran, S. Damarseckin⁶⁴, Z.S. Demiroglu, F. Dolek, C. Dozen⁶⁵, I. Dumanoglu⁶⁶, E. Eskut, G. Gokbulut, Y. Guler, E. Gurpinar Guler⁶⁷, I. Hos⁶⁸, C. Isik, E.E. Kangal⁶⁹, O. Kara, A. Kayis Topaksu, U. Kiminsu, G. Onengut, K. Ozdemir⁷⁰, A. Polatoz, A.E. Simsek, B. Tali⁷¹, U.G. Tok, S. Turkcapar, I.S. Zorbakir, C. Zorbilmez

Middle East Technical University, Physics Department, Ankara, Turkey

B. Isildak⁷², G. Karapinar⁷³, K. Ocalan⁷⁴, M. Yalvac⁷⁵

Bogazici University, Istanbul, Turkey

I.O. Atakisi, E. Gülmез, M. Kaya⁷⁶, O. Kaya⁷⁷, Ö. Özçelik, S. Tekten⁷⁸, E.A. Yetkin⁷⁹

Istanbul Technical University, Istanbul, Turkey

A. Cakir, K. Cankocak⁶⁶, Y. Komurcu, S. Sen⁸⁰

Istanbul University, Istanbul, Turkey

F. Aydogmus Sen, S. Cerci⁷¹, B. Kaynak, S. Ozkorucuklu, D. Sunar Cerci⁷¹

Institute for Scintillation Materials of National Academy of Science of Ukraine, Kharkov, Ukraine

B. Grynyov

National Scientific Center, Kharkov Institute of Physics and Technology, Kharkov, Ukraine

L. Levchuk

University of Bristol, Bristol, United Kingdom

E. Bhal, S. Bologna, J.J. Brooke, E. Clement, D. Cussans, H. Flacher, J. Goldstein, G.P. Heath, H.F. Heath, L. Kreczko, B. Krikler, S. Paramesvaran, T. Sakuma, S. Seif El Nasr-Storey, V.J. Smith, N. Stylianou⁸¹, J. Taylor, A. Titterton

Rutherford Appleton Laboratory, Didcot, United Kingdom

K.W. Bell, A. Belyaev⁸², C. Brew, R.M. Brown, D.J.A. Cockerill, K.V. Ellis, K. Harder, S. Harper, J. Linacre, K. Manolopoulos, D.M. Newbold, E. Olaiya, D. Petyt, T. Reis, T. Schuh, C.H. Shepherd-Themistocleous, A. Thea, I.R. Tomalin, T. Williams

Imperial College, London, United Kingdom

R. Bainbridge, P. Bloch, S. Bonomally, J. Borg, S. Breeze, O. Buchmuller, A. Bundock, V. Cepaitis, G.S. Chahal⁸³, D. Colling, P. Dauncey, G. Davies, M. Della Negra, G. Fedi, G. Hall, G. Iles, J. Langford, L. Lyons, A.-M. Magnan, S. Malik, A. Martelli, V. Milosevic, J. Nash⁸⁴, V. Palladino, M. Pesaresi, D.M. Raymond, A. Richards, A. Rose, E. Scott, C. Seez, A. Shtipliyski, M. Stoye, A. Tapper, K. Uchida, T. Virdee²¹, N. Wardle, S.N. Webb, D. Winterbottom, A.G. Zecchinelli

Brunel University, Uxbridge, United Kingdom

J.E. Cole, P.R. Hobson, A. Khan, P. Kyberd, C.K. Mackay, I.D. Reid, L. Teodorescu, S. Zahid

Baylor University, Waco, USA

S. Abdullin, A. Brinkerhoff, K. Call, B. Caraway, J. Dittmann, K. Hatakeyama, A.R. Kanuganti, C. Madrid, B. McMaster, N. Pastika, S. Sawant, C. Smith, J. Wilson

Catholic University of America, Washington, DC, USA

R. Bartek, A. Dominguez, R. Uniyal, A.M. Vargas Hernandez

The University of Alabama, Tuscaloosa, USA

A. Buccilli, O. Charaf, S.I. Cooper, S.V. Gleyzer, C. Henderson, P. Rumerio, C. West

Boston University, Boston, USA

A. Akpinar, A. Albert, D. Arcaro, C. Cosby, Z. Demiragli, D. Gastler, J. Rohlf, K. Salyer, D. Sperka, D. Spitzbart, I. Suarez, S. Yuan, D. Zou

Brown University, Providence, USA

G. Benelli, B. Burkle, X. Coubez²², D. Cutts, Y.t. Duh, M. Hadley, U. Heintz, J.M. Hogan⁸⁵, K.H.M. Kwok, E. Laird, G. Landsberg, K.T. Lau, J. Lee, M. Narain, S. Sagir⁸⁶, R. Syarif, E. Usai, W.Y. Wong, D. Yu, W. Zhang

University of California, Davis, Davis, USA

R. Band, C. Brainerd, R. Breedon, M. Calderon De La Barca Sanchez, M. Chertok, J. Conway, R. Conway, P.T. Cox, R. Erbacher, C. Flores, G. Funk, F. Jensen, W. Ko[†], O. Kukral, R. Lander, M. Mulhearn, D. Pellett, J. Pilot, M. Shi, D. Taylor, K. Tos, M. Tripathi, Y. Yao, F. Zhang

University of California, Los Angeles, USA

M. Bachtis, R. Cousins, A. Dasgupta, D. Hamilton, J. Hauser, M. Ignatenko, T. Lam, N. Mccoll, W.A. Nash, S. Regnard, D. Saltzberg, C. Schnaible, B. Stone, V. Valuev

University of California, Riverside, Riverside, USA

K. Burt, Y. Chen, R. Clare, J.W. Gary, G. Hanson, G. Karapostoli, O.R. Long, N. Manzanelli, M. Olmedo Negrete, M.I. Paneva, W. Si, S. Wimpenny, Y. Zhang

University of California, San Diego, La Jolla, USA

J.G. Branson, P. Chang, S. Cittolin, S. Cooperstein, N. Deelen, J. Duarte, R. Gerosa, D. Gilbert, V. Krutelyov, J. Letts, M. Masciovecchio, S. May, S. Padhi, M. Pieri, V. Sharma, M. Tadel, F. Würthwein, A. Yagil

University of California, Santa Barbara - Department of Physics, Santa Barbara, USA

N. Amin, C. Campagnari, M. Citron, A. Dorsett, V. Dutta, J. Incandela, B. Marsh, H. Mei, A. Ovcharova, H. Qu, M. Quinnan, J. Richman, U. Sarica, D. Stuart, S. Wang

California Institute of Technology, Pasadena, USA

A. Bornheim, O. Cerri, I. Dutta, J.M. Lawhorn, N. Lu, J. Mao, H.B. Newman, J. Ngadiuba, T.Q. Nguyen, J. Pata, M. Spiropulu, J.R. Vlimant, C. Wang, S. Xie, Z. Zhang, R.Y. Zhu

Carnegie Mellon University, Pittsburgh, USA

J. Alison, M.B. Andrews, T. Ferguson, T. Mudholkar, M. Paulini, M. Sun, I. Vorobiev

University of Colorado Boulder, Boulder, USA

J.P. Cumalat, W.T. Ford, E. MacDonald, T. Mulholland, R. Patel, A. Perloff, K. Stenson, K.A. Ulmer, S.R. Wagner

Cornell University, Ithaca, USA

J. Alexander, Y. Cheng, J. Chu, D.J. Cranshaw, A. Datta, A. Frankenthal, K. Mcdermott, J. Monroy, J.R. Patterson, D. Quach, A. Ryd, W. Sun, S.M. Tan, Z. Tao, J. Thom, P. Wittich, M. Zientek

Fermi National Accelerator Laboratory, Batavia, USA

M. Albrow, M. Alyari, G. Apollinari, A. Apresyan, A. Apyan, S. Banerjee, L.A.T. Bauerdick, A. Beretvas, D. Berry, J. Berryhill, P.C. Bhat, K. Burkett, J.N. Butler, A. Canepa, G.B. Cerati, H.W.K. Cheung, F. Chlebana, M. Cremonesi, V.D. Elvira, J. Freeman, Z. Gecse, E. Gottschalk, L. Gray, D. Green, S. Grünendahl, O. Gutsche, R.M. Harris, S. Hasegawa, R. Heller, T.C. Herwig, J. Hirschauer, B. Jayatilaka, S. Jindariani, M. Johnson, U. Joshi, P. Klabbers, T. Kljnsma, B. Klima, M.J. Kortelainen, S. Lammel, D. Lincoln, R. Lipton, M. Liu, T. Liu, J. Lykken, K. Maeshima, D. Mason, P. McBride, P. Merkel, S. Mrenna, S. Nahn, V. O'Dell, V. Papadimitriou, K. Pedro, C. Pena⁸⁷, O. Prokofyev, F. Ravera, A. Reinsvold Hall, L. Ristori, B. Schneider, E. Sexton-Kennedy, N. Smith, A. Soha, W.J. Spalding, L. Spiegel, S. Stoynev, J. Strait, L. Taylor, S. Tkaczyk, N.V. Tran, L. Uplegger, E.W. Vaandering, H.A. Weber, A. Woodard

University of Florida, Gainesville, USA

D. Acosta, P. Avery, D. Bourilkov, L. Cadamuro, V. Cherepanov, F. Errico, R.D. Field, D. Guerrero, B.M. Joshi, M. Kim, J. Konigsberg, A. Korytov, K.H. Lo, K. Matchev, N. Menendez, G. Mitselmakher, D. Rosenzweig, K. Shi, J. Sturdy, J. Wang, S. Wang, X. Zuo

Florida State University, Tallahassee, USA

T. Adams, A. Askew, D. Diaz, R. Habibullah, S. Hagopian, V. Hagopian, K.F. Johnson, R. Khurana, T. Kolberg, G. Martinez, H. Prosper, C. Schiber, R. Yohay, J. Zhang

Florida Institute of Technology, Melbourne, USA

M.M. Baarmand, S. Butalla, T. Elkafrawy¹⁷, M. Hohlmann, D. Noonan, M. Rahmani, M. Saunders, F. Yumiceva

University of Illinois at Chicago (UIC), Chicago, USA

M.R. Adams, L. Apanasevich, H. Becerril Gonzalez, R. Cavanaugh, X. Chen, S. Dittmer, O. Evdokimov, C.E. Gerber, D.A. Hangal, D.J. Hofman, C. Mills, G. Oh, T. Roy, M.B. Tonjes, N. Varelas, J. Viinikainen, X. Wang, Z. Wu, Z. Ye

The University of Iowa, Iowa City, USA

M. Alhusseini, K. Dilsiz⁸⁸, S. Durgut, R.P. Gandrajula, M. Haytmyradov, V. Khristenko, O.K. Köseyan, J.-P. Merlo, A. Mestvirishvili⁸⁹, A. Moeller, J. Nachtman, H. Ogul⁹⁰, Y. Onel, F. Ozok⁹¹, A. Penzo, C. Snyder, E. Tiras, J. Wetzel

Johns Hopkins University, Baltimore, USA

O. Amram, B. Blumenfeld, L. Corcodilos, M. Eminizer, A.V. Gritsan, S. Kyriacou, P. Maksimovic, C. Mantilla, J. Roskes, M. Swartz, T.Á. Vámi

The University of Kansas, Lawrence, USA

C. Baldenegro Barrera, P. Baringer, A. Bean, A. Bylinkin, T. Isidori, S. Khalil, J. King, G. Krintiras, A. Kropivnitskaya, C. Lindsey, N. Minafra, M. Murray, C. Rogan, C. Royon, S. Sanders, E. Schmitz, J.D. Tapia Takaki, Q. Wang, J. Williams, G. Wilson

Kansas State University, Manhattan, USA

S. Duric, A. Ivanov, K. Kaadze, D. Kim, Y. Maravin, T. Mitchell, A. Modak, A. Mohammadi

Lawrence Livermore National Laboratory, Livermore, USA

F. Rebassoo, D. Wright

University of Maryland, College Park, USA

E. Adams, A. Baden, O. Baron, A. Belloni, S.C. Eno, Y. Feng, N.J. Hadley, S. Jabeen, G.Y. Jeng, R.G. Kellogg, T. Koeth, A.C. Mignerey, S. Nabili, M. Seidel, A. Skuja, S.C. Tonwar, L. Wang, K. Wong

Massachusetts Institute of Technology, Cambridge, USA

D. Abercrombie, B. Allen, R. Bi, S. Brandt, W. Busza, I.A. Cali, Y. Chen, M. D'Alfonso, G. Gomez Ceballos, M. Goncharov, P. Harris, D. Hsu, M. Hu, M. Klute, D. Kovalevskyi, J. Krupa, Y.-J. Lee, P.D. Luckey, B. Maier, A.C. Marini, C. Mcginn, C. Mironov, S. Narayanan, X. Niu, C. Paus, D. Rankin, C. Roland, G. Roland, Z. Shi, G.S.F. Stephans, K. Sumorok, K. Tatar, D. Velicanu, J. Wang, T.W. Wang, Z. Wang, B. Wyslouch

University of Minnesota, Minneapolis, USA

R.M. Chatterjee, A. Evans, P. Hansen, J. Hiltbrand, Sh. Jain, M. Krohn, Y. Kubota, Z. Lesko, J. Mans, M. Revering, R. Rusack, R. Saradhy, N. Schroeder, N. Strobbe, M.A. Wadud

University of Mississippi, Oxford, USA

J.G. Acosta, S. Oliveros

University of Nebraska-Lincoln, Lincoln, USA

K. Bloom, S. Chauhan, D.R. Claes, C. Fangmeier, L. Finco, F. Golf, J.R. González Fernández, C. Joo, I. Kravchenko, J.E. Siado, G.R. Snow[†], W. Tabb, F. Yan

State University of New York at Buffalo, Buffalo, USA

G. Agarwal, H. Bandyopadhyay, C. Harrington, L. Hay, I. Iashvili, A. Kharchilava, C. McLean, D. Nguyen, J. Pekkanen, S. Rappoccio, B. Roozbahani

Northeastern University, Boston, USA

G. Alverson, E. Barberis, C. Freer, Y. Haddad, A. Hortiangtham, J. Li, G. Madigan, B. Marzocchi, D.M. Morse, V. Nguyen, T. Orimoto, A. Parker, L. Skinnari, A. Tishelman-Charny, T. Wamorkar, B. Wang, A. Wisecarver, D. Wood

Northwestern University, Evanston, USA

S. Bhattacharya, J. Bueghly, Z. Chen, A. Gilbert, T. Gunter, K.A. Hahn, N. Odell, M.H. Schmitt, K. Sung, M. Velasco

University of Notre Dame, Notre Dame, USA

R. Bucci, N. Dev, R. Goldouzian, M. Hildreth, K. Hurtado Anampa, C. Jessop, D.J. Kar-mgard, K. Lannon, N. Loukas, N. Marinelli, I. Mcalister, F. Meng, K. Mohrman, Y. Musienko⁴⁷, R. Ruchti, P. Siddireddy, S. Taroni, M. Wayne, A. Wightman, M. Wolf, L. Zygalas

The Ohio State University, Columbus, USA

J. Alimena, B. Bylsma, B. Cardwell, L.S. Durkin, B. Francis, C. Hill, A. Lefeld, B.L. Winer, B.R. Yates

Princeton University, Princeton, USA

B. Bonham, P. Das, G. Dezoort, P. Elmer, B. Greenberg, N. Haubrich, S. Higginbotham, A. Kalogeropoulos, G. Kopp, S. Kwan, D. Lange, M.T. Lucchini, J. Luo, D. Marlow, K. Mei, I. Ojalvo, J. Olsen, C. Palmer, P. Piroué, D. Stickland, C. Tully

University of Puerto Rico, Mayaguez, USA

S. Malik, S. Norberg

Purdue University, West Lafayette, USA

V.E. Barnes, R. Chawla, S. Das, L. Gutay, M. Jones, A.W. Jung, G. Negro, N. Neumeister, C.C. Peng, S. Piperov, A. Purohit, H. Qiu, J.F. Schulte, M. Stojanovic¹⁸, N. Trevisani, F. Wang, A. Wildridge, R. Xiao, W. Xie

Purdue University Northwest, Hammond, USA

T. Cheng, J. Dolen, N. Parashar

Rice University, Houston, USA

A. Baty, S. Dildick, K.M. Ecklund, S. Freed, F.J.M. Geurts, M. Kilpatrick, A. Kumar, W. Li, B.P. Padley, R. Redjimi, J. Roberts[†], J. Rorie, W. Shi, A.G. Stahl Leiton

University of Rochester, Rochester, USA

A. Bodek, P. de Barbaro, R. Demina, J.L. Dulemba, C. Fallon, T. Ferbel, M. Galanti, A. Garcia-Bellido, O. Hindrichs, A. Khukhunaishvili, E. Ranken, R. Taus

Rutgers, The State University of New Jersey, Piscataway, USA

B. Chiarito, J.P. Chou, A. Gandrakota, Y. Gershtein, E. Halkiadakis, A. Hart, M. Heindl, E. Hughes, S. Kaplan, O. Karacheban²⁵, I. Laflotte, A. Lath, R. Montalvo, K. Nash, M. Osherson, S. Salur, S. Schnetzer, S. Somalwar, R. Stone, S.A. Thayil, S. Thomas, H. Wang

University of Tennessee, Knoxville, USA

H. Acharya, A.G. Delannoy, S. Spanier

Texas A&M University, College Station, USA

O. Bouhali⁹², M. Dalchenko, A. Delgado, R. Eusebi, J. Gilmore, T. Huang, T. Kamon⁹³, H. Kim, S. Luo, S. Malhotra, R. Mueller, D. Overton, L. Perniè, D. Rathjens, A. Safonov

Texas Tech University, Lubbock, USA

N. Akchurin, J. Damgov, V. Hegde, S. Kunori, K. Lamichhane, S.W. Lee, T. Mengke, S. Muthumuni, T. Peltola, S. Undleeb, I. Volobouev, Z. Wang, A. Whitbeck

Vanderbilt University, Nashville, USA

E. Appelt, S. Greene, A. Gurrola, R. Janjam, W. Johns, C. Maguire, A. Melo, H. Ni, K. Padeken, F. Romeo, P. Sheldon, S. Tuo, J. Velkovska

University of Virginia, Charlottesville, USA

M.W. Arenton, B. Cox, G. Cummings, J. Hakala, R. Hirosky, M. Joyce, A. Ledovskoy, A. Li, C. Neu, B. Tannenwald, Y. Wang, E. Wolfe, F. Xia

Wayne State University, Detroit, USA

P.E. Karchin, N. Poudyal, P. Thapa

University of Wisconsin - Madison, Madison, WI, USA

K. Black, T. Bose, J. Buchanan, C. Caillol, S. Dasu, I. De Bruyn, P. Everaerts, C. Galloni, H. He, M. Herndon, A. Hervé, U. Hussain, A. Lanaro, A. Loeliger, R. Loveless, J. Madhusudanan Sreekala, A. Mallampalli, D. Pinna, A. Savin, V. Shang, V. Sharma, W.H. Smith, D. Teague, S. Trembath-Reichert, W. Vetens

†: Deceased

- 1: Also at Vienna University of Technology, Vienna, Austria
- 2: Also at Institute of Basic and Applied Sciences, Faculty of Engineering, Arab Academy for Science, Technology and Maritime Transport, Alexandria, Egypt, Alexandria, Egypt
- 3: Also at Université Libre de Bruxelles, Bruxelles, Belgium
- 4: Also at IRFU, CEA, Université Paris-Saclay, Gif-sur-Yvette, France
- 5: Also at Universidade Estadual de Campinas, Campinas, Brazil
- 6: Also at Federal University of Rio Grande do Sul, Porto Alegre, Brazil
- 7: Also at UFMS, Nova Andradina, Brazil
- 8: Also at Universidade Federal de Pelotas, Pelotas, Brazil
- 9: Also at Nanjing Normal University Department of Physics, Nanjing, China
- 10: Also at University of Chinese Academy of Sciences, Beijing, China
- 11: Also at Institute for Theoretical and Experimental Physics named by A.I. Alikhanov of NRC ‘Kurchatov Institute’, Moscow, Russia
- 12: Also at Joint Institute for Nuclear Research, Dubna, Russia
- 13: Also at Helwan University, Cairo, Egypt
- 14: Now at Zewail City of Science and Technology, Zewail, Egypt
- 15: Also at Suez University, Suez, Egypt
- 16: Now at British University in Egypt, Cairo, Egypt
- 17: Now at Ain Shams University, Cairo, Egypt
- 18: Also at Purdue University, West Lafayette, USA
- 19: Also at Université de Haute Alsace, Mulhouse, France
- 20: Also at Erzincan Binali Yildirim University, Erzincan, Turkey
- 21: Also at CERN, European Organization for Nuclear Research, Geneva, Switzerland
- 22: Also at RWTH Aachen University, III. Physikalisches Institut A, Aachen, Germany
- 23: Also at University of Hamburg, Hamburg, Germany
- 24: Also at Department of Physics, Isfahan University of Technology, Isfahan, Iran, Isfahan, Iran
- 25: Also at Brandenburg University of Technology, Cottbus, Germany
- 26: Also at Skobeltsyn Institute of Nuclear Physics, Lomonosov Moscow State University, Moscow, Russia
- 27: Also at Institute of Physics, University of Debrecen, Debrecen, Hungary, Debrecen, Hungary
- 28: Also at Physics Department, Faculty of Science, Assiut University, Assiut, Egypt
- 29: Also at MTA-ELTE Lendület CMS Particle and Nuclear Physics Group, Eötvös Loránd University, Budapest, Hungary, Budapest, Hungary
- 30: Also at Institute of Nuclear Research ATOMKI, Debrecen, Hungary

- 31: Also at IIT Bhubaneswar, Bhubaneswar, India, Bhubaneswar, India
- 32: Also at Institute of Physics, Bhubaneswar, India
- 33: Also at G.H.G. Khalsa College, Punjab, India
- 34: Also at Shoolini University, Solan, India
- 35: Also at University of Hyderabad, Hyderabad, India
- 36: Also at University of Visva-Bharati, Santiniketan, India
- 37: Also at Indian Institute of Technology (IIT), Mumbai, India
- 38: Also at Deutsches Elektronen-Synchrotron, Hamburg, Germany
- 39: Also at Sharif University of Technology, Tehran, Iran
- 40: Also at Department of Physics, University of Science and Technology of Mazandaran, Behshahr, Iran
- 41: Now at INFN Sezione di Bari ^a, Università di Bari ^b, Politecnico di Bari ^c, Bari, Italy
- 42: Also at Italian National Agency for New Technologies, Energy and Sustainable Economic Development, Bologna, Italy
- 43: Also at Centro Siciliano di Fisica Nucleare e di Struttura Della Materia, Catania, Italy
- 44: Also at Università di Napoli 'Federico II', Napoli, Italy
- 45: Also at Riga Technical University, Riga, Latvia, Riga, Latvia
- 46: Also at Consejo Nacional de Ciencia y Tecnología, Mexico City, Mexico
- 47: Also at Institute for Nuclear Research, Moscow, Russia
- 48: Now at National Research Nuclear University 'Moscow Engineering Physics Institute' (MEPhI), Moscow, Russia
- 49: Also at Institute of Nuclear Physics of the Uzbekistan Academy of Sciences, Tashkent, Uzbekistan
- 50: Also at St. Petersburg State Polytechnical University, St. Petersburg, Russia
- 51: Also at University of Florida, Gainesville, USA
- 52: Also at Imperial College, London, United Kingdom
- 53: Also at P.N. Lebedev Physical Institute, Moscow, Russia
- 54: Also at INFN Sezione di Padova ^a, Università di Padova ^b, Padova, Italy, Università di Trento ^c, Trento, Italy, Padova, Italy
- 55: Also at Budker Institute of Nuclear Physics, Novosibirsk, Russia
- 56: Also at Faculty of Physics, University of Belgrade, Belgrade, Serbia
- 57: Also at Trincomalee Campus, Eastern University, Sri Lanka, Nilaveli, Sri Lanka
- 58: Also at INFN Sezione di Pavia ^a, Università di Pavia ^b, Pavia, Italy, Pavia, Italy
- 59: Also at National and Kapodistrian University of Athens, Athens, Greece
- 60: Also at Universität Zürich, Zurich, Switzerland
- 61: Also at Ecole Polytechnique Fédérale Lausanne, Lausanne, Switzerland
- 62: Also at Stefan Meyer Institute for Subatomic Physics, Vienna, Austria, Vienna, Austria
- 63: Also at Laboratoire d'Annecy-le-Vieux de Physique des Particules, IN2P3-CNRS, Annecy-le-Vieux, France
- 64: Also at Şırnak University, Sirnak, Turkey
- 65: Also at Department of Physics, Tsinghua University, Beijing, China, Beijing, China
- 66: Also at Near East University, Research Center of Experimental Health Science, Nicosia, Turkey
- 67: Also at Beykent University, Istanbul, Turkey, Istanbul, Turkey
- 68: Also at Istanbul Aydin University, Application and Research Center for Advanced Studies (App. & Res. Cent. for Advanced Studies), Istanbul, Turkey
- 69: Also at Mersin University, Mersin, Turkey
- 70: Also at Piri Reis University, Istanbul, Turkey
- 71: Also at Adiyaman University, Adiyaman, Turkey
- 72: Also at Ozyegin University, Istanbul, Turkey
- 73: Also at Izmir Institute of Technology, Izmir, Turkey
- 74: Also at Necmettin Erbakan University, Konya, Turkey
- 75: Also at Bozok Universitetesi Rektörlüğü, Yozgat, Turkey, Yozgat, Turkey

- 76: Also at Marmara University, Istanbul, Turkey
- 77: Also at Milli Savunma University, Istanbul, Turkey
- 78: Also at Kafkas University, Kars, Turkey
- 79: Also at Istanbul Bilgi University, Istanbul, Turkey
- 80: Also at Hacettepe University, Ankara, Turkey
- 81: Also at Vrije Universiteit Brussel, Brussel, Belgium
- 82: Also at School of Physics and Astronomy, University of Southampton, Southampton, United Kingdom
- 83: Also at IPPP Durham University, Durham, United Kingdom
- 84: Also at Monash University, Faculty of Science, Clayton, Australia
- 85: Also at Bethel University, St. Paul, Minneapolis, USA, St. Paul, USA
- 86: Also at Karamanoğlu Mehmetbey University, Karaman, Turkey
- 87: Also at California Institute of Technology, Pasadena, USA
- 88: Also at Bingol University, Bingol, Turkey
- 89: Also at Georgian Technical University, Tbilisi, Georgia
- 90: Also at Sinop University, Sinop, Turkey
- 91: Also at Mimar Sinan University, Istanbul, Istanbul, Turkey
- 92: Also at Texas A&M University at Qatar, Doha, Qatar
- 93: Also at Kyungpook National University, Daegu, Korea, Daegu, Korea